frontiers | Frontiers in Earth Science

TYPE Original Research
PUBLISHED 05 October 2022
DOI 10.3389/feart.2022.967201

Check for updates

OPEN ACCESS

EDITED BY
Yihuai Zhang,
Imperial College London,
United Kingdom

REVIEWED BY
Nisar Ahmed,
University of Stavanger, Norway
Souvik Sen,
Halliburton Inc., United States
Chao Li,
Institute of Geology and Geophysics (CAS), China
Shib Ganguli,
National Geophysical Research Institute (CSIR), India

*CORRESPONDENCE
Ahmed E. Radwan,
radwanae@yahoo.com

SPECIALTY SECTION
This article was submitted to Economic Geology,
a section of the journal
Frontiers in Earth Science

RECEIVED 12 June 2022
ACCEPTED 12 August 2022
PUBLISHED 05 October 2022

CITATION
Radwan AE (2022), A multi-proxy approach to detect the pore pressure and the origin of overpressure in sedimentary basins: An example from the Gulf of Suez rift basin.
Front. Earth Sci. 10:967201.
doi: 10.3389/feart.2022.967201

COPYRIGHT
© 2022 Radwan. This is an open-access article distributed under the terms of the Creative Commons Attribution License (CC BY). The use, distribution or reproduction in other forums is permitted, provided the original author(s) and the copyright owner(s) are credited and that the original publication in this journal is cited, in accordance with accepted academic practice. No use, distribution or reproduction is permitted which does not comply with these terms.

A multi-proxy approach to detect the pore pressure and the origin of overpressure in sedimentary basins: An example from the Gulf of Suez rift basin

Ahmed E. Radwan*

Faculty of Geography and Geology, Institute of Geological Sciences, Jagiellonian University, Kraków, Poland

The pore pressure gradient and fracture gradient (PPFG) are critical parameters for drilling mud weight design in the energy industry. Successful drilling operations can be achieved successfully through the understanding of the pore pressure and fracture pressure in the subsurface succession. The scope of this research is to use an integrated approach that encompasses well-logging, basin modeling, drilling-based interpretations, and reservoir measurement methods to gain a reasonable PPFG model and decrease the drilling uncertainties in the El Morgan oil field in the Gulf of Suez. Moreover, it investigates the overpressure generation mechanisms in the basin, which have not been studied before in this area. In this work, PPFGs of more than 16 km of cumulative thick sedimentary succession were modeled and evaluated using an integrated approach. This study utilizes Eaton's sonic and resistivity-based methods for pore pressure evaluation, while vertical stress was calculated based on the composite density profile. The study revealed that the top geo-pressure was detected at a depth of 1,030 m of Tortonian sediments. Late Miocene sediments reveal hard over-pressure with a maximum gradient of 0.55 PSI/feet, while Middle Miocene sediments exhibit mildly over-pressured, normal, and sub-normal pore pressure zones. The lowest pore pressure values were measured in the Langhian-Serravalian Kareem reservoir with a gradient of 0.29 PSI/feet. With the exception of a slight difference in the reservoir section, the pore pressure profiles in the northern and southern parts of the El Morgan oil field are relatively similar. Reservoir connectivity is believed to be the main reason behind pore pressure magnitude differentiation in the Middle Miocene reservoirs. The key mechanism for generating overpressure has been identified as disequilibrium compaction, and reservoir overcharging may contribute as an excess-pressure generation mechanism at the reservoir level. The presented approach can be applied in PPFG studies for both development and exploratory geomechanical studies in other areas of the Gulf of Suez basin or elsewhere in the world.

KEYWORDS

pore pressure, overpressure generation mechanisms, disequilibrium compaction, fracture pressure, basin modeling, overpressure, pore pressure gradient and fracture gradient, gulf of Suez

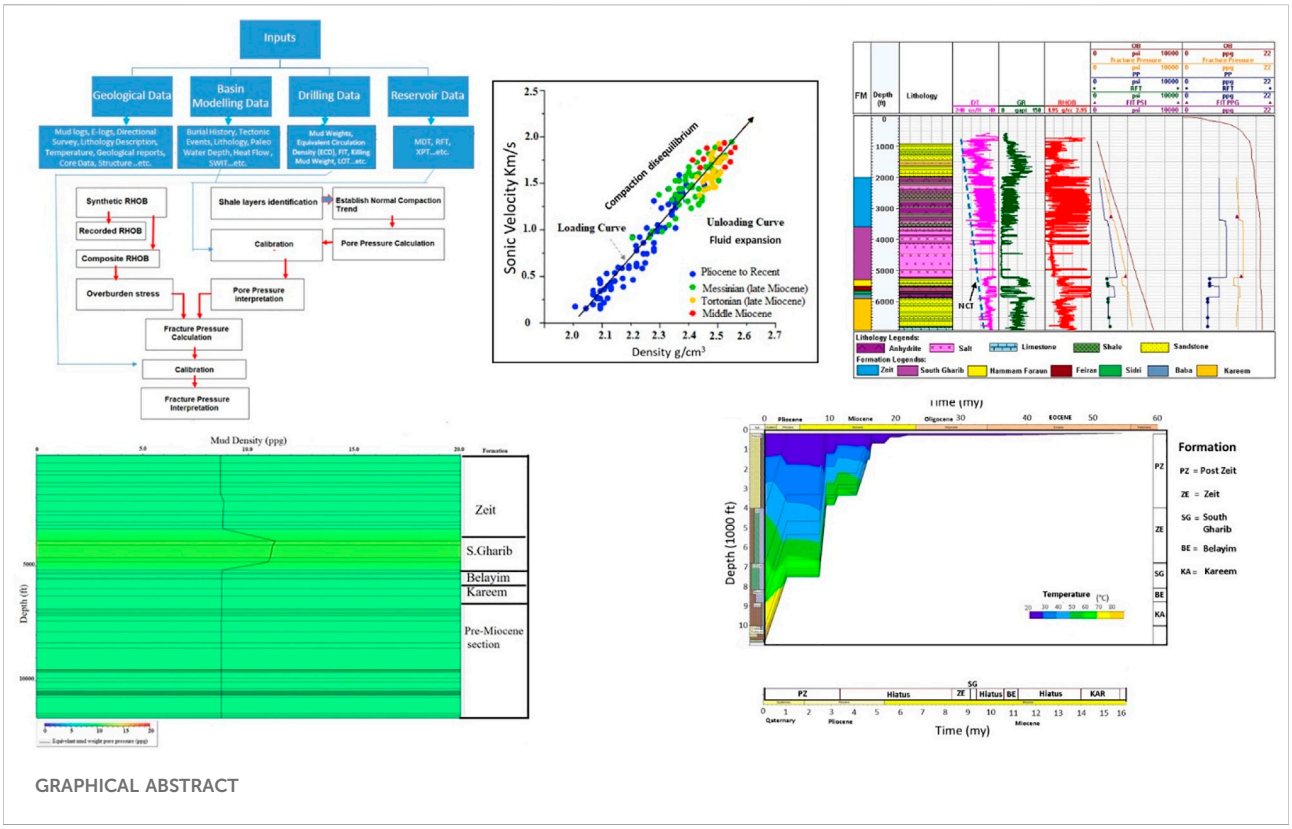

GRAPHICAL ABSTRACT

Introduction

Abnormal pore pressure is one of the main challenges for drilling engineers and exploration geologists, and it can be sub-classified into overpressure and sub-normal pressure (Figure 1) (e.g., Bourgoyne et al., 1986; Mouchet and Mitchele, 1989; Neuzil, 1995; Yassir and Bell, 1996; Osborne and Swarbrick, 1997; Sayers et al., 2002; Ramdhan and Goulty, 2010; Ramdhan and Goulty, 2011; Zhang, 2011; Radwan et al., 2019a; Radwan et al., 2020a; Radwan, 2021b). Overpressure generation mechanisms (Figure 2) have been studied in many sedimentary basins, and they are linked with disequilibrium compaction (e.g., Martinsen, 1994; Hart et al., 1995; Klaus, 1999; Vejbæk, 2008; Kumar and Rao, 2012; Marín-Moreno et al., 2013; Wang et al., 2016; Drews et al., 2019; Zhang et al., 2019; Li et al., 2021), clay diagenesis (e.g., Jeans, 1994; Lahann et al., 2001; Katahara, 2006; Lahann and Swarbrick, 2011), tectonic activities (e.g., Hao et al., 2004; Luo et al., 2007), hydrocarbon generation (Spencer, 1987; Osborne and Swarbrick, 1997; Hansom and Lee, 2005; Chi et al., 2010), and thermal effects (e.g., Mello and Karner, 1996; He et al., 2002).

Historically and despite decades of research into the subsurface sediment characteristics, it remains difficult to predict critical reservoir parameters of strata buried in sedimentary basins such as pore pressure (e.g., Gretener, 1979; Audet and McConnell, 1992; Martinsen, 1994; Gordon and Flemings, 1998; Dutta, 2002; Chopra and Huffman, 2006; Gutierrez et al., 2006; Zhang, 2011; Radwan et al., 2019b; Baouche et al., 2020a; Radwan et al., 2020a; Baouche et al., 2020b; Ganguli and Sen, 2020; Radwan and Sen, 2021a; Radwan, 2021b; Radwan and Sen, 2021b) and fracture pressure (e.g., Anderson et al., 1973; Traugott, 1997; Draou and Osisanya, 2000; Radwan et al., 2019b; Sen and Ganguli, 2019; Tariq et al., 2019; Radwan et al., 2020a; Radwan, 2021b). The importance of pore pressure and fracture pressure is related to their influence on drilling operations (e.g., Gray-Stephens et al., 1994; Swarbrick, 2012; Sen et al., 2020; Abdelghany et al., 2021; Radwan, 2021b), exploration (e.g., O'connor et al., 2011a; John et al., 2014), and reservoir stability and production (e.g., Hillis, 2000; Agbasi et al., 2021; Radwan and Sen, 2021a; Radwan and Sen, 2021b; Kassem et al., 2021).

In the oil and gas industry, pore pressure is measured in reservoirs using specific tools (i.e., bottom-hole pressure gauge, well testing), and it can be predicted or estimated using indirect methods (Radwan et al., 2019b). Pore pressure can be measured in permeable zones (e.g., Swarbrick, 2002; Dasgupta et al., 2016; Sen et al., 2017; Adouani et al., 2019; Radwan et al., 2019b; Dasgupta et al., 2019; Radwan et al., 2020a; Radwan, 2021b). On the other hand, seismic velocities (e.g., Sayers et al., 2002; Chopra and Huffman, 2006; Bachrach et al., 2007; Khan et al., 2017; Hussain and Ahmed, 2018), well logs (e.g., Zhang, 2011;

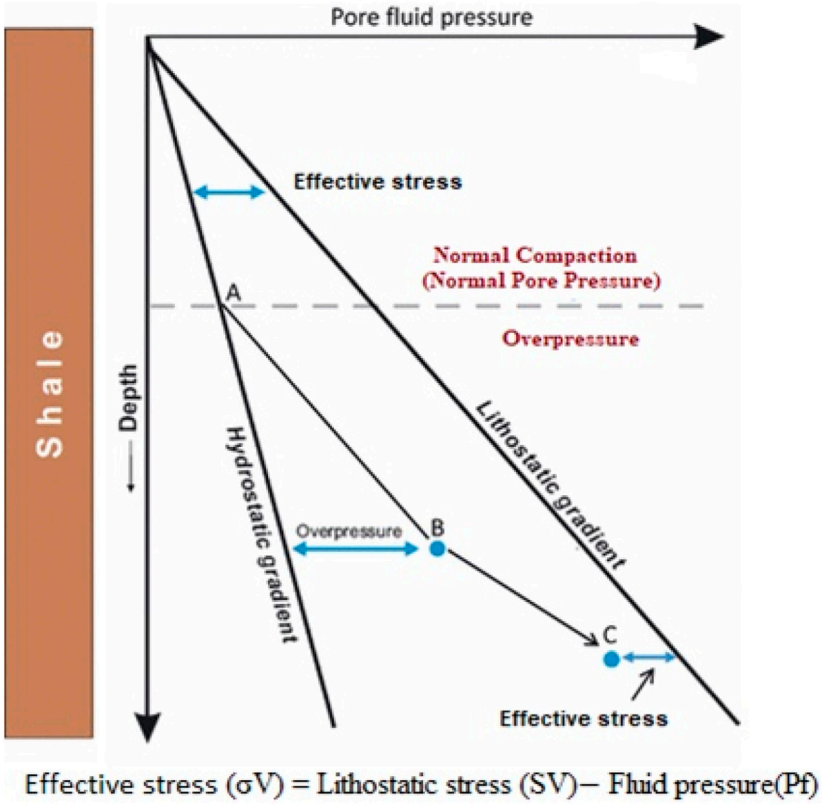

FIGURE 1
Cartoon illustration showing the definitions of overpressure (deviation from hydrostatic) and Terzaghi (simple) vertical effective stress (σV=SV–Pf).

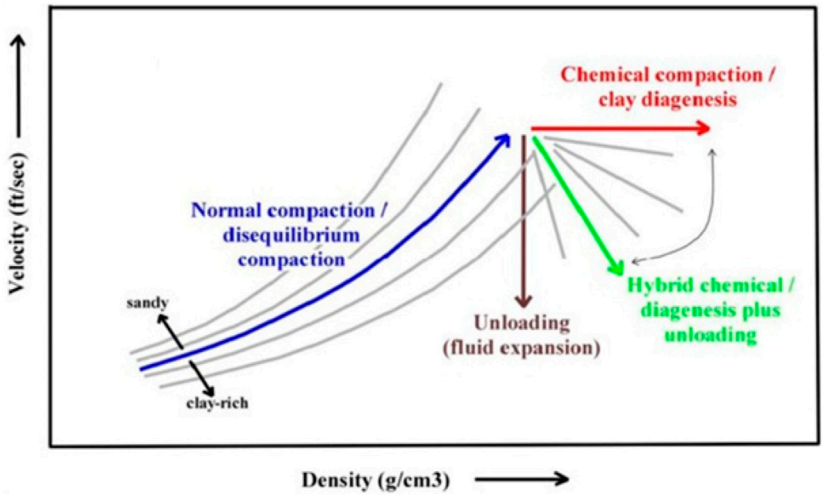

FIGURE 2
Typical curve-types from velocity-density cross plots with associated overpressure generating mechanisms (Hoesni, 2004).

Wessling et al., 2013; Radwan et al., 2019b) and basin modeling (e.g., Nordgård Bolås et al., 2004; Radwan et al., 2020a; Li et al., 2022) are used to predict and estimate pore pressure in frontier sedimentary basins. Drilling parameters and well logs can be used for pressure estimation while drilling (e.g., Mouchet and Mitchele, 1989; Zhang, 2011; Peters et al., 2017; Bourgoyne et al., 1991; Alam et al., 2019). Standard methods, including effective-depth methods and empirical methods (e.g., Eatons' method, Bowers' method), have been used for pore pressure prediction in the industry. However, these methods have been used with fair success in areas like the Gulf of Mexico, where sedimentation rates are fairly rapid. Applying these methods in other areas, e.g., the North Sea and the Gulf of Suez, has been more problematic due to the differences in the used parameters and geological conditions (Law and Spencer, 1998; Helset et al., 2009; Shaker, 2015; Snee, 2015; Radwan et al., 2019b; Radwan, 2021b). However, many researchers rely solely on one method for interpreting pore pressures, which may not be efficient in some areas. Recently, researchers have applied machine learning to predict pore pressure in sedimentary basins (e.g., Ahmed et al., 2019; Jafarizadeh et al., 2022; Radwan et al., 2022), as well as 3D modeling being used in pore pressure modeling (e.g., Lopez et al., 2004; Altmann et al., 2014; Radwan, 2022a; Chen et al., 2022).

Reviewing the previous literature on pore pressure prediction and detection methods suggests that geophysical logging has been used for pore pressure prediction in many basins globally (e.g., Eaton, 1975; Traugott, 1997; Bowers, 2001). Reservoir measurements have been used for PPFG model calibration and as direct measurement methods (e.g., Drews et al., 2018; Radwan, 2018; Sen et al., 2019, Sen et al., 2020; Radwan, 2021b). Also, drilling events can be utilized to calibrate the pore pressure model (e.g., Zhang, 2011; Brahma et al., 2013; Das and Chatterjee, 2018a; Das and Chatterjee, 2018b; Radwan et al., 2019b; Mahetaji et al., 2019; Radwan et al., 2020a). In addition, basin modeling has been considered as the primary tool for pressure prediction in frontier areas. Basin modeling results can give a clear image of sedimentation rate, tectonics, erosion, etc., which consequently affect the geopressure mechanism (e.g., Thomsen, 1998; Darby et al., 1998; Bjørlykke et al., 2010; Karlsen and Skeie, 2006; Couzens-Schultz and Azbel, 2014; Snee, 2015; Satti, et al., 2015; Burgreen-Chan et al., 2015; Peters et al., 2017; Mosca et al., 2018; Nagy et al., 2019; Radwan et al., 2020a). However, there is no preferred method that could guarantee and be commonly accepted as better than another method. Therefore, the capability of integrating most of the previously mentioned methods can provide a higher degree of confidence for the predicted pore pressure fracture gradient (PPFG) model.

The Gulf of Suez basin is classified as one of the challenging basins in terms of drilling due to complex tectonic and structural settings (Radwan, 2018; Abass et al., 2019; Radwan et al., 2019b; Radwan et al., 2020a; Radwan, 2021b). However, to date, overpressure generation mechanisms have not been studied before in the Gulf of Suez basin, despite their importance and implications for drilling activity. In this work, the proposed approach relies on the integration of more than one method to obtain the most appropriate PPFG model for the studied basin area of El Morgan field. Basin modeling, reservoir, and drilling data were used as additional inputs with geophysical logging for pore pressure prediction and calibration in the studied oil field. The integration of the previously mentioned tools can drive exemplary modeling of the geopressure. Also, overpressure generation mechanisms in the Gulf of Suez basin were investigated in this work, which have not been studied before and may have implications for the overpressure prediction process, and consequently achieving successful drilling in the studied area. The prime objectives of this work are to: 1) detect the overpressure generation mechanism in the El Morgan area that has not been investigated before in the rift basin, 2) present an improved integrated workflow approach that can act as a valuable reference case in sedimentary basins using combined methods, 3) extend our knowledge of the pore pressure distribution in the penetrated formations of the studied area, and 4) highlight the pore pressure regimes and geopressure zones within the entire (Middle Miocene to recent) sequence.

Geologic setting and lithostratigraphy

The Gulf of Suez rift basin (Figure 3) is an iconic offshore basin that formed in the Oligocene-Miocene period, and lies in the northwest branch of the Red Sea. As evidenced by geophysical and borehole data, the basin is filled with more than a 5-km-thick sedimentary sequence ranging from the Precambrian to the Quaternary (Metwalli et al., 1981; Metwalli et al., 1982; El-Hattab, 1982; Montenat et al., 1988; EGPC, 1996; Radwan, 2022b), which is punctuated by several unconformities of different magnitudes and ages (Figure 3). The studied area of El Morgan oil field is situated in the south central offshore area of the rift basin, where numerous hydrocarbon plays are present (Figure 3) (Alsharhan and Salah, 1995; EGPC, 1996; Bosworth and McClay, 2001; Barakat et al., 2002; Youssef et al., 2002; Alsharhan, 2003; Radwan, 2014; Attia et al., 2015; Abudeif et al., 2016a; El Ayouty, 2017; Abudeif et al., 2018; Radwan, 2018; Radwan et al., 2019a; Radwan et al., 2019b; Radwan et al., 2019c; Radwan et al., 2020a; Radwan et al., 2020b; Radwan et al., 2020c; Radwan et al., 2021a; Radwan et al., 2021b; Radwan et al., 2021c; Radwan et al., 2021d; Radwan et al., 2021e; Ali et al., 2022). El Morgan field is located on the southwest coast of the Sinai Peninsula, covering an area of roughly 46 km^2 (Bentley and Biller, 1990; Radwan, 2014; Attia et al., 2015). El Morgan field is classified as the biggest giant oil field in Egypt with more than 1.5 BBO reserves. The stratigraphic sequence of El Morgan oil field is classified into three main depositional mega sequences, namely pre-rift, syn-rift, and post-rift (Brown, 1980; Attia et al.,

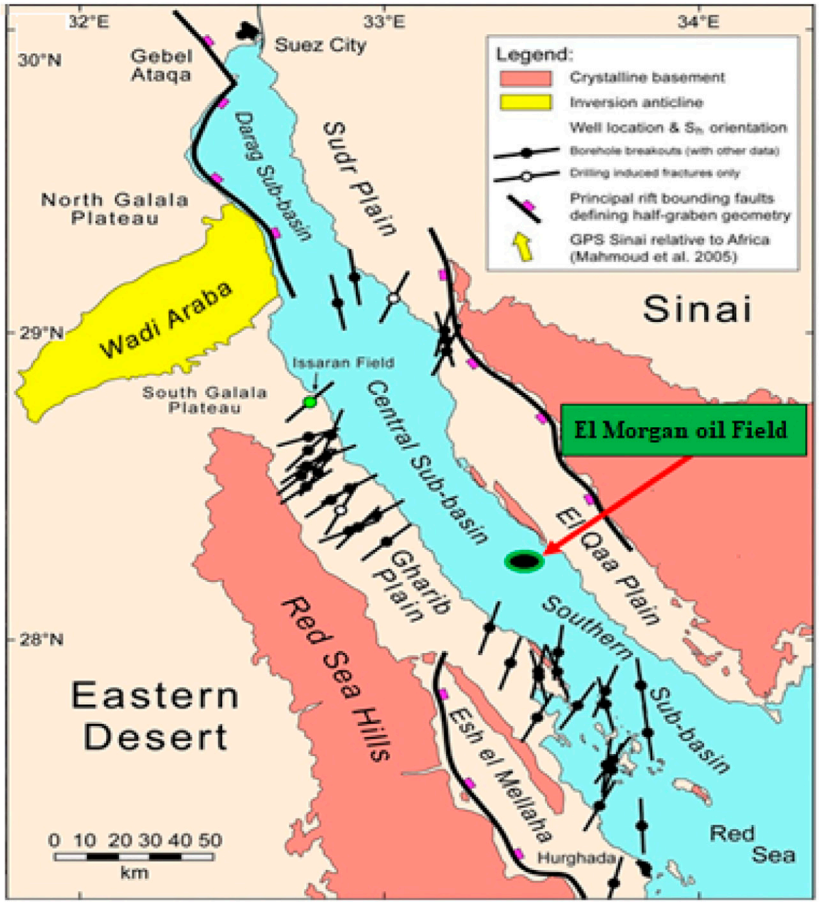

FIGURE 3
Location map of the Gulf of Suez and the El Morgan oil field (adopted from Mahmoud et al., 2005; Bosworth and Taviani 1996; Bosworth and Durocher 2017).

2015; Abudeif et al., 2016a; Abudeif et al., 2016b; Radwan et al., 2019b; Radwan et al., 2019c; Radwan, 2021a; Radwan et al., 2021a; Radwan, 2021b; Radwan et al., 2021b; Radwan, 2021c; Radwan et al., 2021c; Radwan et al., 2021d; Radwan et al., 2021e). The deposition of sediments in the study area took place in different depositional environments (EGPC, 1996). Two main sandstone reservoirs were deposited during the syn-rift time. The Kareem Formation and Belayim Formation (Hammam Faraun Member) (Figure 4) are typical of a fan delta depositional environment (El-Ashry, 1972; EGPC, 1996; Hughes et al., 1997). Miocene sandstone rocks are the main reservoir rocks, and they trap hydrocarbons that originate from the organic-rich carbonate (Campanian-Maastrichtian and Eocene), shales (Paleocene), and marls (Miocene) (Brown, 1980; Rohrback, 1982; Barakat et al., 1997; AlSharahan, 2003; El Nady, 2006; El Diasty and Peters, 2014). The thick evaporites of the Miocene section are the sealing rocks in the area (AlSharahan, 2003; Radwan, 2014; Radwan et al., 2021c).

The tectonic evolution of this area is linked to the tilted fault block system in the rift basin (Robson, 1971; Patton et al., 1994; Schutz, 1994; Bosworth et al., 1998; Radwan et al., 2020b; Moustafa and Khalil, 2020). The field structure is a NW-SE trending, anticlinal, horst block, with dips of <6–8° (Figure 5) (Gawad et al., 1986; Khalil and Meshrif, 1988; Rashed, 1990; EGPC, 1996; Alsharhan, 2003; Jackson et al., 2006; Ali et al., 2016; Radwan, 2018; Radwan et al., 2019b; Radwan et al., 2021c). The El Morgan oil field is divided into the north and south portions by the El Morgan hinge zone (Figure 5). The studied A well is located in the northern part of the field, while the H well is located in the southern part of the field, as shown in Figure 5.

Materials and methods

The data of eight offshore wells that represent the northern and southern parts of the El Morgan field were used in the execution of this work. The studied wells are named (A, B, C, D,

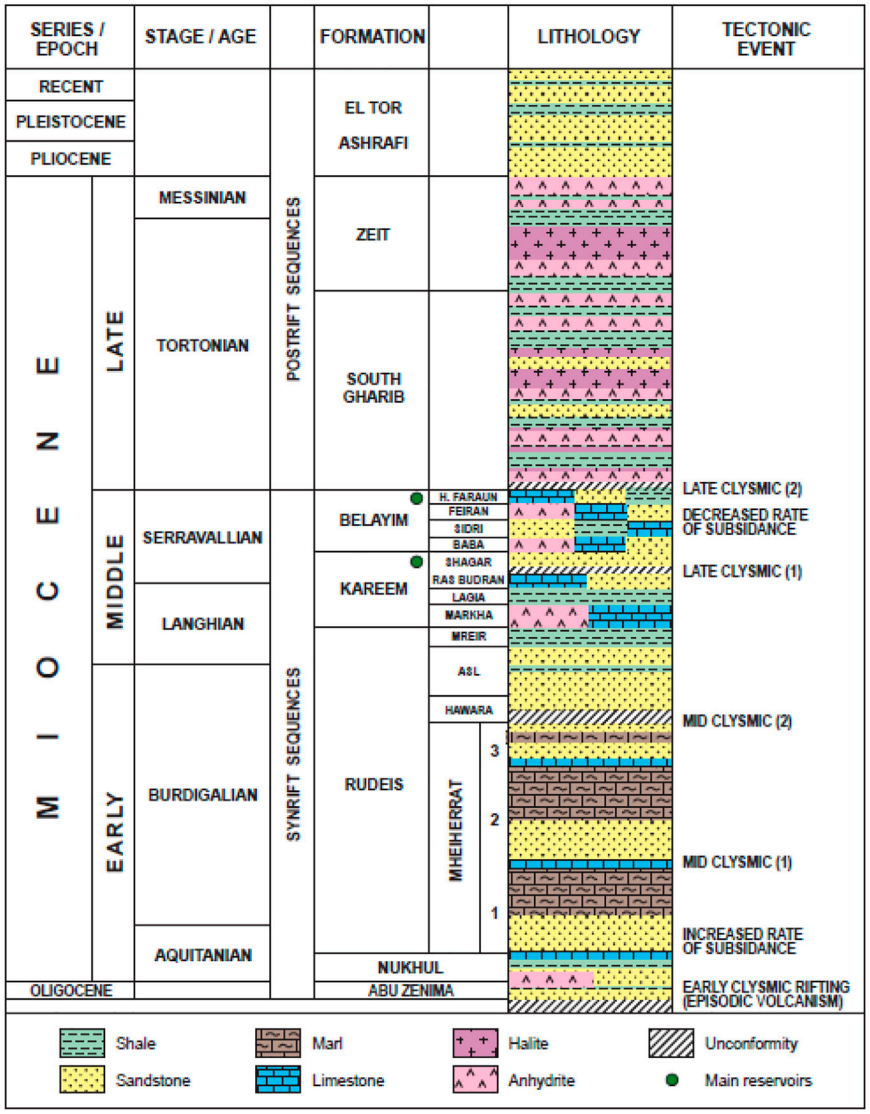

FIGURE 4
Stratigraphy and lithology of the El Morgan oil field (Radwan, 2018).

E, F, G, and H). Wells A and B were used for modeling, while other wells' data were used as offset wells (Figure 5). All available data, including a high-resolution geophysical log suite consisting of gamma, resistivity, formation bulk density, and sonic logs, were the key inputs for this study.

Vertical stress and pore pressure

The weight of the overburden rock is called vertical stress (σV) or overburden (Plumb et al., 1991; Shaker, 2007; Paul et al., 2009; Zhang 2011). The composite density profile (Eq. 1) was utilized for overburden stress calculations in the region using available data (Radwan et al., 2020a; Radwan, 2021b). Finite data in the topmost part of the surface section in the studied wells was considered a severe challenge in this study. The Amoco density method was utilized to count the pseudodensity in the surface section (Eq. 2) (Paul et al., 2009; Radwan et al., 2019b). The estimated density from the Amoco equation was appended to the wireline density logs, and hence the composite density profile was developed for the studied wells (Plumb et al., 1991; Matthews, 2004; Radwan et al., 2019b).

The vertical stress gradient (OBG) calculation applying the Amoco method can be expressed by Eq. 1:

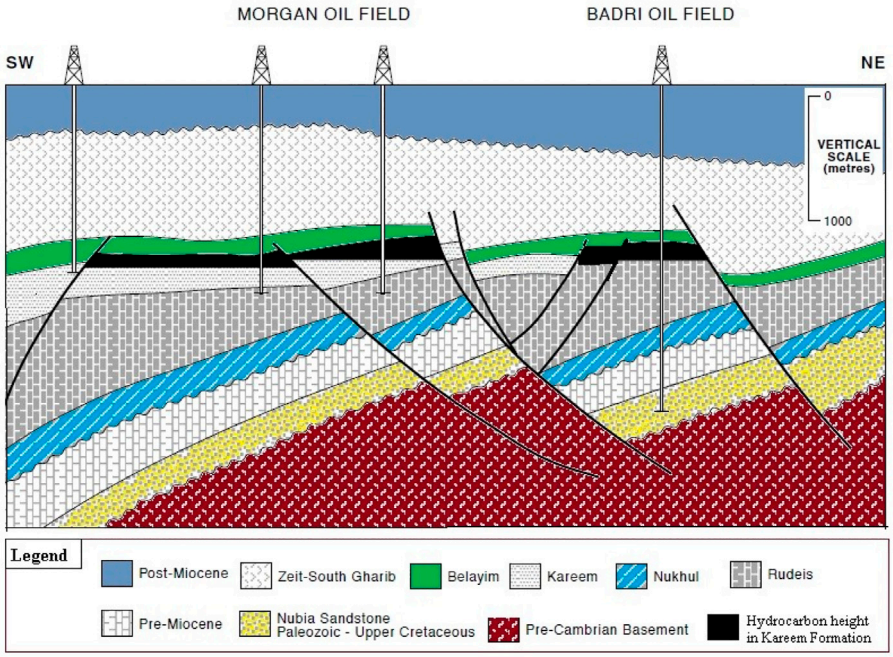

FIGURE 5
Generalized SW-NE cross-section showing the stratigraphy and structural relationship of the El Morgan field (Radwan, 2022b).

$$Sv = \int_0^Z RHOB(Z) * g\, dZ \quad (1)$$

$$\sigma V\ Amoco = \sigma mudline + ((TVD - AG - WD)/3125)\alpha \quad (2)$$

The hydrostatic pressure in the area of the Gulf of Suez is equivalent to 8.7 (pounds per gallon) (Selim et al., 2003; Selim and Badawy, 2010; Radwan, 2018; Radwan et al., 2019b; Radwan et al., 2020a; Radwan, 2021b). The identification of shale zones in this study is based on well logs and lithology descriptions. The normal compaction trend (NCT) was considered as the hydrostatic pressure which is equivalent to 8.7 (pounds per gallon) (Radwan, 2018; Radwan et al., 2019b; Radwan et al., 2020a). Eaton's sonic and resistivity methods were used to estimate the pore pressure from the eight wells (Eqs 3, 4) (Eaton, 1975).

$$PP = OBG - (OBG - PPN)\left(\frac{Ro}{Rnx}\right)^x \quad (3)$$

$$PP = OBG - (OBG - PPN)\left(\frac{\Delta To}{\Delta Tn}\right)^x \quad (4)$$

Fracture pressure

The fracture pressure was determined using the Eaton fracture method (Eaton, 1975). The fracture pressure was calibrated with the formation integrity test (FIT) data from the studied wells to check the fracture pressure profile. The previously used Poisson's ratio in the Gulf of Suez was used in this study (Selim et al., 2003; Selim and Badawy, 2010; Radwan et al., 2019b; Radwan et al., 2020a; Radwan et al., 2020b). The fracture pressure equation is expressed as the following:

$$F = Sv - D/P(v/1 - v) + (P/D) \quad (5)$$

Burial history modeling and drilling events

1D basin modeling has been created for the sedimentary section of the studied field using Schlumberger's PetroMod© (V. 2018). The bottom hole temperature was estimated from 1D basin modeling and validated by the actual measured temperature in the wells using the Horner method (Kutasov and Eppelbaum, 2005). The stratigraphic section used in building the basin model is based on the biostratigraphic and lithostratigraphic approaches in the area of El Morgan Field, which has thick Miocene sediments (Radwan, 2021b). Furthermore, internal biostratigraphic and geological lithostratigraphic reports from the literature were used to build the representative history model (Radwan A. E., 2021-Radwan, 2021c; Radwan et al., 2021a-Radwan et al., 202e). The measured

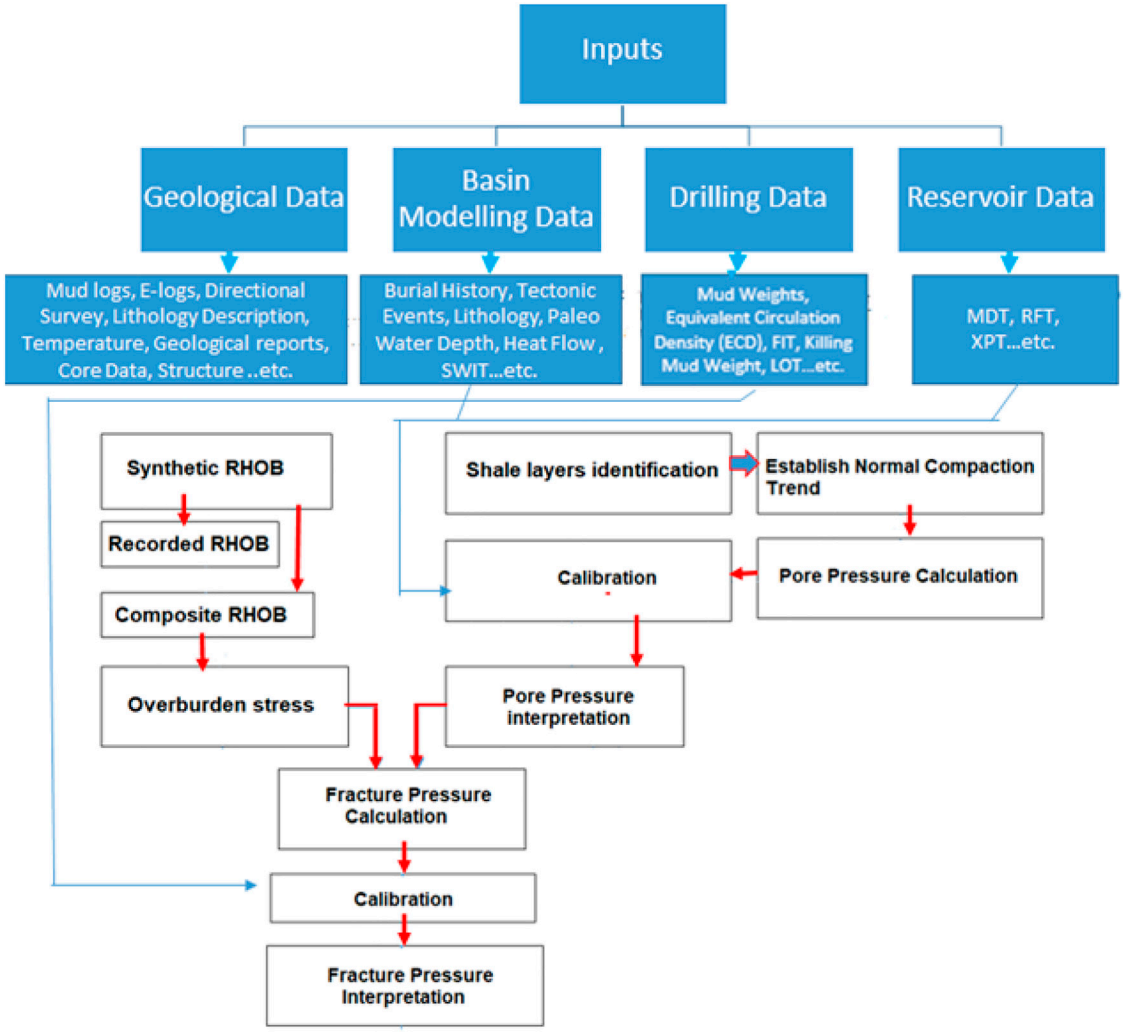

FIGURE 6
Pore pressure evaluation workflow.

bottom hole temperature data was used to validate the thermal history model for the two wells, and the measured data of vitrinite organic matter reflectance (% VRo) was utilized to calibrate the model. The temperature history of the sediments along with the wells and burial history modeling were created by basin modeling software that was provided by Gulf of Suez petroleum company (GUPCO). Sedimentation history, deposition timing, and formation age were the key inputs into basin modeling for the geopressured zones. In addition, drilling events and reservoir pressure were employed to validate the PPFG model output results. Schlumberger charts were used for environmental corrections for the logging data set (Charts, 1991). Overpressure generation mechanisms in El Morgan oil field were inferred from the relation between sonic velocity and density (Hoesni, 2004).

The proposed multidisciplinary geopressure evaluation workflow

The proposed multidisciplinary PPFG analysis workflow is dependent mainly on the integration of indirect methods (geophysical methods), measured reservoir data, and drilling event-based interpretations. In addition, basin modeling is integrated with the previous methods, where it represents an effective tool for sedimentation rate determination and overpressure prediction. This workflow goes through five procedures: a) data collection, b) summarizing the data and quality control, 3) calculation process, 4) model result calibration, and 5) final model results. Geophysical data, basin modeling, drilling data, and reservoir measurements are the primary inputs in this approach (Figure 6).

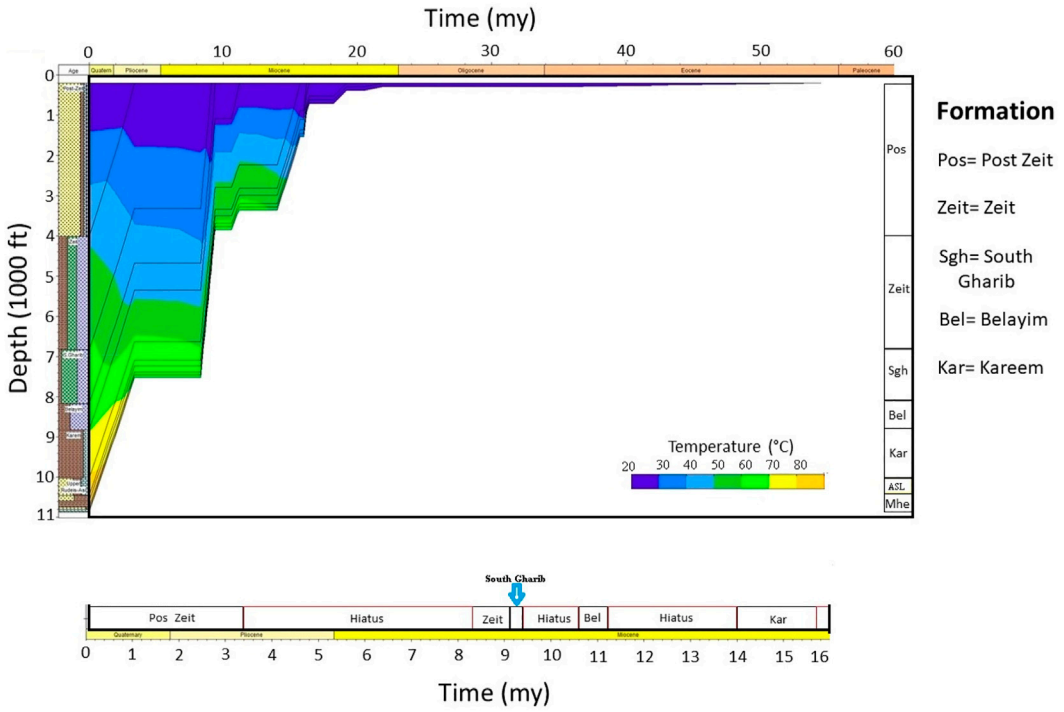

FIGURE 7
The burial history model for well A presents the thermal burial history evolution with time and rate of deposition.

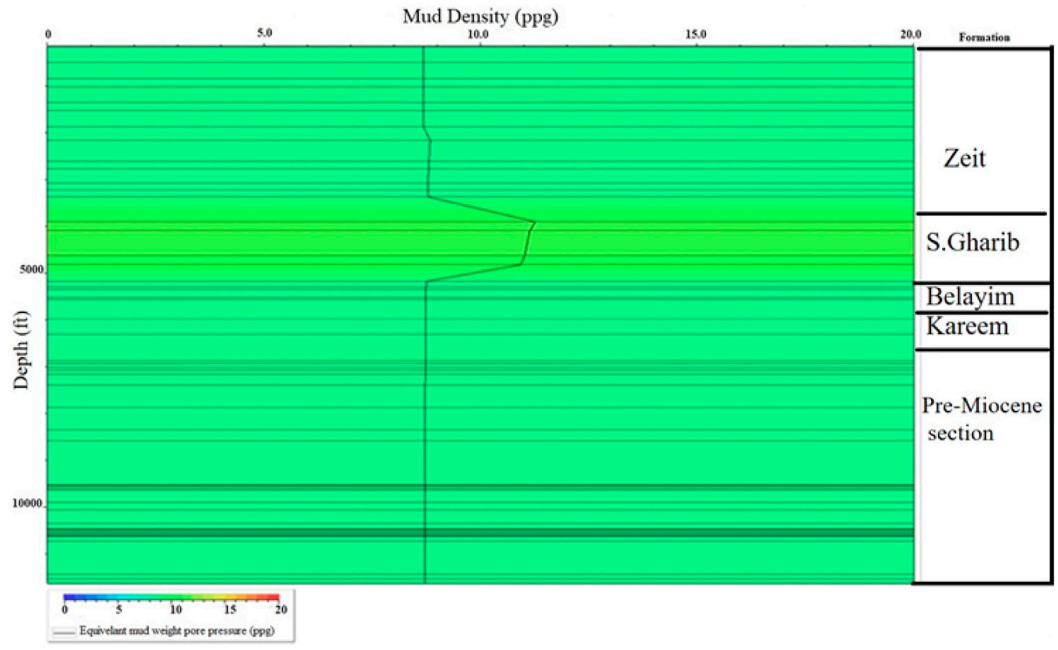

FIGURE 8
1D basin modeling represents the conversion of burial history into equivalent mud weight versus the depth in feet per each formation.

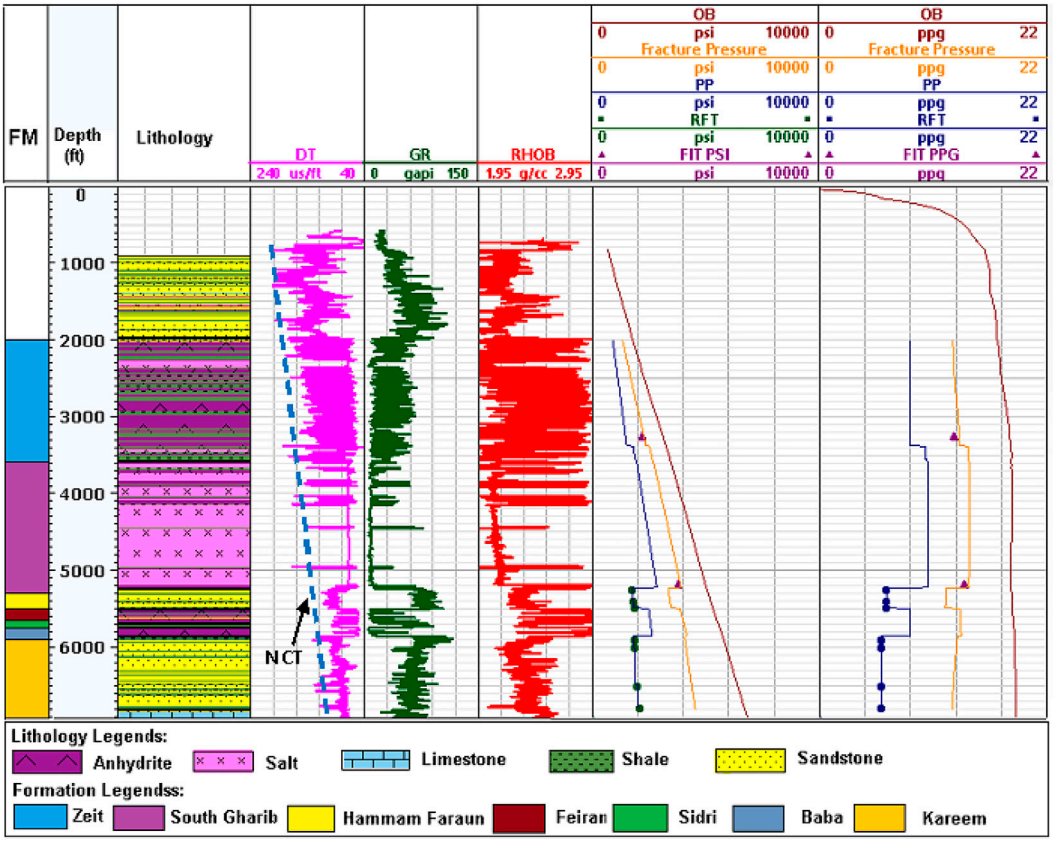

FIGURE 9
PPFG model output of in the El Morgan oil field.

Results and discussion

In this study, the studied well logs cover more than 16 km (cumulative well logs) and represent eight wells in the El Morgan oil field, with each well having a thickness of about 2 km. The results of basin modeling, pore pressure, fracture pressure, and overpressure generation mechanisms are discussed as follows:

Basin modeling

Basin modeling, according to Duppenbecker et al. (2004) and Radwan et al. (2020a), can be used to predict and understand pressure evolution or porosity anomaly expectations. Integration of geological, geophysical, and geochemical data allows for establishing a sequential record of basin history changes through the sedimentation process (Poelchau et al., 1997; Thomsen, 1998). As a result, basin modeling can be used as the main key indicator as a quantitative tool for pore pressure prediction, in addition to routine petroleum system evaluation. Moreover, understanding the sedimentation history in the basin can lead to enhancing the abnormal pressure prediction.

The penetrated subsurface section of the El Morgan oil field contains sediments from the Langhian to the Quaternary periods (Figure 4). The developed burial history for the studied field has been converted to equivalent pressure mud density using the PetroMod© (V. 2018). In this study, a thermal history for well A was constructed (Figure 7). In the Gulf of Suez, the temperature history is controlled by the heat flow and subsidence generated by the clysmic tectonic events during rifting stages (Prosser, 1993). The temperature was estimated using 1D basin modeling and confirmed using the actual bottom hole temperature (Figure 7) calculated using the generalized Horner method (Kutasov and Eppelbaum, 2005). Consequently, the constructed one-dimensional burial history for the studied area indicated high sedimentation rates which generated overpressure in the late Miocene formations (South Ghraib and Zeit). Following the relation between depth in feet versus the equivalent pressure density within the sediment for each formation, equivalent pressure build-up was detected against the base of Zeit and South Ghraib formations up to 10.5 ppg (Figure 8).

TABLE 1 Studied wells drilling summary model, where the drilling problems listed per each formation are accompanied by the rig operation during drilling events and actions.

Formation name	Well name	Drilling problems	Operation
ZEIT	A, C, G, and H	Partial losses	Drilling
	A and E	Hole fill	tripping
	A, F, C, and B	Tight spot	Tripping
	A and H	Caved shale	Drilling
South Gharib	A, D, E, and G	Salt creeping	Tripping
	A and F	well flow	Drilling
Belayim	A, C, G, and H	Partial losses	Drilling
Kareem	A, C, G, and H	Tight spot partial losses	Tripping

TABLE 2 PPFG model values in the field, where (OVB) is the overburden pressure, (FRAC) is the fracture pressure, and (PP) is the pore pressure in ppg units. Maximum pore pressure of the Hammam Faraun and Kareem reservoirs represents the shale pore pressure.

WELL	Formation	OVB		FRAC		PP		Pressure regime
		Min ppg	Max ppg	Min ppg	Max ppg	Min ppg	Max ppg	
A	ZEIT	17.17	18.54	12.85	14.34	8.65	10.30	*Normal pore pressure
								*Over pressurized
	S.GHARIB	18.49	18.57	14.21	14.46	10.50	10.50	*Over pressurized
	H.FARAUN	18.54	18.57	12.17	12.27	6.5	9.4	*Sub-normal pore pressure
								*Over pressurized
								Reservoir pressure based on repeated formation test, maximum is the virgin reservoir pressure
	FEIRAN	18.62	18.73	13.57	13.62	8.7	8.7	*Normal pore pressure
	SIDRI	18.75	18.76	13.63	13.64	8.7	8.7	*Normal pore pressure
	BABA	18.78	18.85	13.65	13.68	8.7	8.7	*Normal pore pressure
	KAREEM	18.88	18.98	12.83	13.27	6	9.4	*Sub-normal
								*Over pressurized
								Reservoir pressure based on repeated formation test
								Maximum is the virgin reservoir pressure

More than 700 m (2,296 feet) of sediments were buried in the El Morgan oil field in less than 3 million years during the Tortonian and Messinian periods, indicating a high tendency for compaction disequilibrium to occur in the late Miocene sediments. Figure 8 shows the relation between depth in feet with the equivalent pressure density within the sediment for each formation; the base of the Zeit formation and the South Ghraib formation showed equivalent pressure build-up of more than 10.5 ppg (Figure 8). Pore pressure predictions show that the overpressure is showing a significant deviation in the interval between 975 m (3,200 feet) and 1,525 m (5,000 feet). This fast sedimentation process gives a build-up of overpressure that reflects disequilibrium compaction of the shale due to the high sedimentation rate and fast sediment burial. To properly interpret and predict pore pressure at the studied oil field, velocity and density must be investigated for overpressure generation mechanisms detection. The results of basin modeling analysis in El Morgan oil field are relatively similar to the results of the neighboring Badri oil field, where they have relatively the same geological conditions.

Vertical stress, pore pressure, and fracture pressure analysis

In the investigated eight wells, overburden or vertical stress was found to have an average of 18 ppg equivalent mud weight (EMW) (Figure 9). The overburden gradient increases from

TABLE 3 Calculated magnitudes (PSI) and gradients (PSI/feet) of overburden (OB), fracture pressure (FP), and pore pressure (PP).

Depth	Formation	PP		FP		OB		Comments
		Magnitude	Gradient	Magnitude	Gradient	Magnitude	Gradient	
Feet		PSI	PSI/feet	PSI	PSI/feet	PSI	PSI/feet	
2110	Zeit	954	0.45	1,420	0.67	1901	0.90	FIT at base 0.68 PSI/feet
2510		1,134	0.45	1704	0.68	2292	0.91	
3010		1,360	0.45	2090	0.69	2843	0.94	
3585		1955	0.54	2692	0.74	3452	0.96	
3610	South Gharib	1967	0.55	2710	0.75	3475	0.96	FIT at base 0.73 PSI/feet
4010		2187	0.55	3014	0.75	3867	0.96	
4510		2460	0.55	3391	0.75	4351	0.96	
5215		2844	0.55	3914	0.75	5016	0.96	
5310	Hammam Faraun	1800	0.34	3382	0.64	5116	0.96	Depleted reservoir, Virgin PP 0.50 PSI/feet
5410		1810	0.34	3431	0.64	5214	0.96	
5490		1825	0.34	3471	0.64	5296	0.96	
5610	Feiran	2534	0.45	3967	0.71	5443	0.97	Mainly anhydrite
5670		2562	0.45	4018	0.71	5519	0.97	
5700	Sidri	2574	0.45	4040	0.71	5551	0.97	Mainly shale
5730		2588	0.45	4063	0.71	5583	0.97	
5770	Baba	2607	0.45	4097	0.71	5633	0.98	Mainly anhydrite
5840		2633	0.45	4146	0.71	5704	0.98	
5910	Kareem	1700	0.29	4082	0.69	5795	0.98	Depleted reservoir, Virgin PP 0.49 PSI/feet
6010		1715	0.29	4133	0.69	5899	0.98	
6510		1720	0.29	4381	0.69	6403	0.98	
6810		1726	0.29	4527	0.69	6699	0.98	

0.91 PSI/feet at the top of the Zeit Formation to 0.98 PSI/feet at the base of the Kareem Formation. The compressional slowness was able to detect the overpressure zone through the late Miocene sediments in the absence of resistivity log. Measured reservoir pressure data was used in the interpretation and calibration of the PPFG model. On the other hand, all encountered drilling problems were documented in Table 1, which was used as an indicator for excess pressure.

The pore pressure started as normal pressure with 0.45 PSI/feet at sea bed sediments to the Zeit Formation, then the pore pressure gradient increased by 0.09 PSI/feet and reached 0.54 PSI/feet at a depth of 1,030 m. Pore pressure development continued in the Turonian sediments and reaches up to 0.54 PSI/feet. Most of the Serravalian Belayim Formation prevailed normal pore pressure with a gradient of 0.45 PSI/feet except the top part that has the reservoir interval (Hammam Faraun Member). The Hammam Faraun Member sandstone shows subnormal conditions based on reservoir measurements with a gradient of 0.34 PSI/feet. Reservoir measurements show a subnormal condition in the Kareem Formation with a gradient of 0.29 PSI/feet. Mild-overpressure was developed in the Serravalian shales and reaches up to 9.4 ppg with a gradient of 0.50 and 0.49 PSI/feet in the Hammam Faraun and Kareem Formations, in an arrangement. The current pore pressure, overburden stress, and fracture pressure dataset of El Morgan oil field was documented in Tables 2, 3. Table 2 shows the results in ppg equivalent mud weight, while Table 3 shows the results in PSI/feet. The pore pressure and fracture pressure were modeled in this work to reflect the shale and sandstone pressures, but it does not reflect the pore pressure in other lithologies.

The studied eight wells are classified as development wells, which were drilled through the explored middle Miocene reservoirs in the El Morgan block. Several drilling complexities in terms of salt creeping, tight spots, losses, formation fluid influxes, and wellbore failures are observed in the studied wells. The interpreted PP indicated that the top part of the sediments from the sea bed till late Miocene age sediments display hydrostatic pore pressure equal to 8.7 ppg (EMW). At the base of the Zeit formation and starting from a depth of 1,030 m (3,379 feet) to the base of the South Gharib formation (Tortonian), sonic log response deviates from the NCT, this zone indicating hard overpressure. In addition, two influx events

were reported from these layers and the kill mud weight was considered in the PP interpretation (Table 1). The interpreted PP in the base of the Zeit Formation is equal to 10.3 ppg (EMW), while it is equal to 10.5 ppg (EMW) in the South Gharib Formation. Because this zone is a sandstone reservoir zone, PP gives misleading values when using Eaton's equation at the top of the Belayim Formation (i.e., the Hammam Faraun Member). Therefore, PP interpretation of this reservoir zone was solely based on measured (MDT) data. Prolonged production and depletion have reduced the PP to sub-hydrostatic levels, with pore pressures of 6.5 ppg (EMW) and a gradient of 0.34 PSI/feet. On the other hand, the shale intervals indicated mild overpressure equivalent to 9.4 ppg (EMW), hence it still keeps the virgin pressure of the reservoir (2537 PSI) at a depth of 1,554 m (5100 feet) with a gradient of 0.50 PSI/feet. The three members of the Belayim Formation (Feiran, Sidri, and Baba) display normal hydrostatic conditions with a gradient of 0.45 PSI/feet. The middle Miocene (Kareem Formation) shows subnormal conditions, and the sandstone reservoir pore pressure is 6 ppg (EMW) with a gradient of 0.29 PSI/feet, while it comprises mild overpressure in the shale intervals equivalent to 9.4 ppg (EMW). Therefore, it still keeps the virgin pressure of the reservoir (2990 PSI) at a depth of 1859 m (6100 feet) with a gradient of 0.49 PSI/feet.

Fracture pressure was estimated from Eq. 3, and it shows matching with the FIT data (Figure 9). Fracture pressure gradient decreases against the depleted middle Miocene reservoirs and possesses a risk of fracturing if a higher mud pressure is used while drilling. Digital numbers of the estimated overburden, pore pressure, and fracture pressure were documented in Tables 2, 3. Figure 9 represents the PPFG model output of the studied wells. Sandstone PP only is drawn in the reservoirs section. When the pore pressure profiles of the northern (A, B, C, and D) and southern (E, F, G, and H) El Morgan oil field wells are compared, the pore pressure is the same for all formations except the middle Miocene reservoir sections. It should be noted that pore pressure magnitude differentiation in the Middle Miocene reservoirs is related to reservoir connectivity, where the studied wells are located in different compartmentalizations within the field (Figure 5).

Overpressure generation mechanisms

The mudstone compaction trends are slowed or even stopped by disequilibrium compaction, but they do not deviate from them. On the other hand, fluid expansion or overpressure transfer can lead to unloading, which will result in a sonic transit time reversal and little response in density (Figure 2). Disequilibrium compaction during rapid sedimentation of sediments is one of the main mechanisms that contributed to the development of non-hydrostatic conditions in low-permeability layers in the Gulf of Mexico,

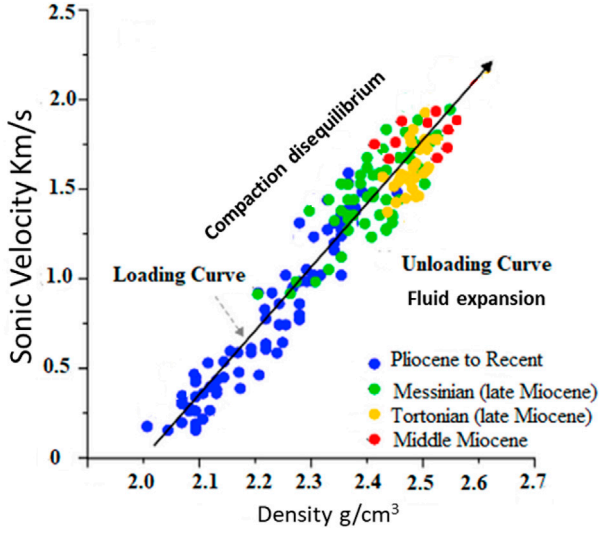

FIGURE 10
Cross plot of velocity and density for the studied wells.

Australia, South Caspian Basin, Asia, and the North Sea (e.g., Swarbrick and Osborne, 1998; Lee et al., 1999; Carcione and Gangi, 2000; Gutierrez and Wangen, 2005; Berhmann et al., 2006; O'Connor et al., 2011a; O'Connor et al., 2011b). This mechanism is applicable when fluids cannot be expelled out of the fine-grained sediments due to vertical compaction, and consequently, the entrapment fluids will share in the sediment load. The magnitude of abnormal pressure, in this case, is related to permeability, or how the entrapment fluids will move within the rock pores considering the balance between the continuous creation of PP by sediment loading. It is expected that the degree of abnormal overpressure tends to develop at greater depths based on the expected significant decrease in permeability at deeper depths (Neuzil and Pollock, 1983; Marín-Moreno et al., 2013; Luo and Vasseur, 1996).

Other excess-pressure mechanisms are attributed to fluid phase changes and diagenesis of clay minerals (Swarbrick and Osborne, 1998). The diagenetic process of clay illitization occurs at temperatures ranging from 80°C to 150°C (Nadeau, 1985), but the maximum temperature at the Kareem reservoir is 78°C, excluding this process as a candidate for the overpressure generation mechanism in the studied field. Lateral compression is usually common in compressional basins (McPherson and Garven, 1999; Xie et al., 2001), which is not the case here, where the investigated basin is an extensional rift basin, so this process has been also excluded in this case. The reservoir overcharging mechanism (Grauls and Baleix, 1993) was considered in this case as a potential contributor to the overpressure generation. In the El Morgan field, fluid movement from source rocks to the field reservoirs was proven as up-dip migration from the Campanian-

Maastrichtian source rocks to the Miocene reservoirs through faults (EGPC, 1996; Radwan et al., 2021c; Radwan, 2022b), which could increase the pore pressure and develop excess pressure in the reservoirs. In such a case, fluid volume and charging rate are the main controlling factors of the overpressure value. In addition, drainage efficiency, pore and fluid compressibility, and reservoir extension all contribute to the generated overpressure value or magnitude. The overpressure magnitude was increased by 0.7 ppg (0.05 and 0.04 PSI/feet) at the reservoir levels, which could be called low-overpressure (Xie et al., 2001). To gain a better understanding of the overpressure generation mechanism in the El Morgan oil field, the density vs. sonic velocity was plotted as per previous studies (Figure 10) (Swarbrick and Osborne 1998; Hoesni, 2004; O'Conner et al., 2011a; O'Conner et al., 2011b; Lahann and Swarbrick 2011). From the cross-plot, disequilibrium compaction was interpreted as the main mechanism that generates overpressure across the Miocene sediments in the El Morgan oil field (Figure 10). The plotted points remain on the loading curve, suggesting that overpressure in the El Morgan oil field is generated by disequilibrium compaction. The plot results are indicative that the higher sedimentation rate in the late and middle Miocene was responsible for retaining the connate water in the shales and thus exerting hard overpressure. Based on the previous plot results, it is inferred that disequilibrium compaction is the main overpressure generation mechanism in the studied area, while the reservoir overcharging mechanism could contribute to the overpressure generation mechanism with lower magnitude at the level of the studied reservoirs.

Model uncertainty

The variable burial history of the Gulf of Suez encompasses varying timings and magnitudes of sediment burial, uplift, and hiatus from one area to another. Because of the high variability of the sedimentation conditions, predicting pore pressures is difficult, and evaluating pore pressures is prone to uncertainty. For the studied case, the results were calibrated by the multi-available data, and the estimated pore pressure showed good matching between geophysical and basin modeling analysis of the late Miocene shales, where both of them indicated 10.5 ppg (EMW). On the other hand, there is no uncertainty related to the middle Miocene reservoirs, where it represents the actual measured data for both sandstone intervals as direct measurements and shale intervals as indirect measurements based on the equilibrium theory. Acceptable uncertainty can be found along the stratigraphic section in the studied field, but with no or few implications on the developed PPFG model based on the multi-proxy approach. Hence, the integration of multidisciplinary data from geology, geophysics, reservoirs, and drilling can decrease the uncertainties and lead to a more reliable PPFG model.

Basin modeling, geophysical logging, drilling events based interpretations, and reservoir data integration outstanding features

Pore pressure prediction in exploratory and development wells depends mainly on seismic and basin modeling methods. Once the first well in an oil field has been drilled, well logs are commonly recorded along the drilled section. Geophysical logging data can be used to estimate pore pressure in sedimentary basin drilled wells (Eaton, 1975; Bowers, 2001; Zhang, 2011). Pore pressure estimation using well logging works primarily in mud-rocks, but direct measurement in reservoir sections can also provide accurate pore pressure data in subsurface sandstone rocks. Considering the pressure equilibrium between sand and shale in the virgin basins, measured reservoir data, in this case, is equal to shale pore pressure (Yardley and Swarbrick, 2000; Daniel, 2001). Basin modeling and burial history development are widely used tools for simulating hydrocarbon generation and sedimentation processes that contribute to overpressure distribution (e.g., Mudford et al., 1991; Borge, 2002; Nordgård Bolås et al., 2004; Hansom and Lee, 2005). As a result, basin modeling is the primary tool for providing an informative vision and understanding of sedimentary basin developments, indicating high potential abnormal pressure zones before going through calculation methods to infer pressure magnitudes. Drilling events-based interpretations can help in the calibration process, and it is considered one of the key elements in the PPFG evaluation process, where it represents the actual observations inside the drilled wells (Bowers, 2001; Radwan et al., 2019b). Using one method can result in overestimated or underestimated results, which will have a negative impact on the final PPFG model and deliver high uncertainties in the developed PPFG model.

The developed approach in this work can be applied in PPFG studies for both development and exploratory geomechanical studies within other fields of the Gulf of Suez basin or elsewhere in the world. The presented approach has the advantage of being a multidisciplinary approach that integrates the geological basin analysis, recorded logs, drilling problem based interpretations, and reservoir measurement data to enhance the understanding of subsurface pore pressure behavior in a specific region. Consequently, the benefits of this integrated data are the following: 1) The proposed integrated pore pressure evaluation approach could lead to a boost in the pore pressure evaluation process; 2) it has the potential to reduce the uncertainty of the geopressure model and lead to a more

accurate one; and 3) it has the potential to aid in the determination of more reliable casing seats, which has implications for successful drilling operations. The limitation of this approach is the lack of any tool from previously collected data, which may be the case in many regions, making the PPFG development less accurate to some extent.

Conclusion

- ✓ The current study introduces a multi-proxy approach to predicting the PPFG model in sedimentary basins, using the El Morgan oil field as a case study.
- ✓ According to PPFG analysis, normal PP was detected in the Messinian to recent zone and the Serravalian sediments of (Feiran, Sidri, and Baba) members. Hard overpressure was detected in the Tortonian sediments.
- ✓ The first mild overpressure was detected in the mudstone interval of the Hammam Faraun Member, and the second mild overpressure was detected in the mudstone interval of the Kareem Formation. The main hydrocarbon producing reservoirs, i.e., middle Miocene (sandstone), showed sub-hydrostatic pressure conditions that most likely resulted from production-related depletion.
- ✓ Pore pressure magnitude differentiation in the Middle Miocene reservoirs is most likely related to reservoir connectivity, where the studied wells are located in different compartmentalizations within the field.
- ✓ Compaction disequilibrium was identified as a key mechanism for generating mild overpressure in the studied basin; however, reservoir overcharging may also contribute as a mechanism at the reservoir level.
- ✓ The presented approach has the advantage of being a multidisciplinary approach that integrates the geological basin analysis, recorded logs, drilling problems-based interpretations, and reservoir measurements data to improve understanding of subsurface pore pressure behavior in the study area.
- ✓ By using multi-proxy integrated data, the presented approach could reduce the uncertainty of the geopressure model and lead to an adequate one, as well as assist in the determination of more reliable casing seats, which has implications for drilling activities.
- ✓ This approach could be applied in PPFG studies for both development and exploratory geomechanical studies within other fields of the Gulf of Suez Basin or elsewhere in the world.

Data availability statement

The original contributions presented in the study are included in the article/supplementary material, and further inquiries can be directed to the corresponding author.

Author contributions

The author confirms being the sole contributor of this work and has approved it for publication.

Funding

The publication was funded by the Priority Research Area Anthropocene under the program "Excellence Initiative—Research University" at the Jagiellonian University in Kraków.

Acknowledgments

The author is grateful to the Gulf of Suez Petroleum Company (GUPCO) and the Egyptian Petroleum Corporation (EGPC) authorities for providing the required data and their permissions to proceed with this research, GUPCO provided the software during the author work at the company. The author is thankful to the four reviewers who reviewed the manuscript and provided constructive comments to improve the paper. The publication was funded by the Priority Research Area Anthropocene under the program "Excellence Initiative—Research University" at the Jagiellonian University in Krakow.

Conflict of interest

The author declares that the research was conducted in the absence of any commercial or financial relationships that could be construed as a potential conflict of interest.

Publisher's note

All claims expressed in this article are solely those of the authors and do not necessarily represent those of their affiliated organizations, or those of the publisher, the editors and the reviewers. Any product that may be evaluated in this article, or claim that may be made by its manufacturer, is not guaranteed or endorsed by the publisher.

References

Abass, A. E., Teama, M. A., Kassab, M. A., and Elnaggar, A. A. (2019). Integration of mud logging and wire-line logging to detect overpressure zones: a case study of middle Miocene Kareem Formation in ashrafi oil field, gulf of suez, Egypt. *J. Pet. Explor Prod. Technol.*, 1–21.

Abudeif, A., Attia, M., and Radwan, A. (2016a). New simulation technique to estimate the hydrocarbon type for the two untested members of Belayim Formation in the absence of pressure data, Badri Field, Gulf of Suez, Egypt. *Arab. J. Geosci.* 9 (3), 218–221. doi:10.1007/s12517-015-2082-2

Abudeif, A., Attia, M., and Radwan, A. (2016b). Petrophysical and petrographic evaluation of Sidri member of Belayim Formation, Badri field, gulf of suez, Egypt. *J. Afr. Earth Sci.* 115, 108–120. doi:10.1016/j.jafrearsci.2015.11.028

Abudeif, A. M., Attia, M. M., Al-Khashab, H. M., and Radwan, A. E. (2018). Hydrocarbon type detection using the synthetic logs: A case study, Baba member, gulf of suez, Egypt. *J. Afr. Earth Sci.* 144, 176–182. doi:10.1016/j.jafrearsci.2018.04.017

Adouani, S., Ahmadi, R., Khlifi, M., Akrout, D., Mercier, E., and Montacer, M. (2019). Pore pressure assessment from well data and overpressure mechanism: Case study in Eastern Tunisia basins. *Mar. Georesources Geotechnol.*, 1–14. doi:10.1080/1064119X.2019.1633711

Agbasi, O. E., Sen, S., Inyang, N. J., and Etuk, S. E. (2021). Assessment of pore pressure, wellbore failure and reservoir stability in the Gabo field, Niger Delta, Nigeria-Implications for drilling and reservoir management. *J. Afr. Earth Sci.* 173, 104038. doi:10.1016/j.jafrearsci.2020.104038

Ahmed, A., Elkatatny, S., Ali, A., Mahmoud, M., and Abdulraheem, A. (2019). New model for pore pressure prediction while drilling using artificial neural networks. *Arab. J. Sci. Eng.* 44 (6), 6079–6088. doi:10.1007/s13369-018-3574-7

Alam, J., Chatterjee, R., and Dasgupta, S. (2019). Estimation of pore pressure, tectonic strain and stress magnitudes in the upper Assam basin: a tectonically active part of India. *Geophys. J. Int.* 216 (1), 659–675. doi:10.1093/gji/ggy440

Ali, Kh.A., Abd Elrazik, E. E. D., Azam, S. Sh., and Saleh, A. H. (2016). Integrated petrophysical and lithofacies studies of lower-middle Miocene reservoirs in Belayim marine oil field, Gulf of Suez, Egypt. *J. Afr. Earth Sci.* 117, 331–344. doi:10.1016/j.jafrearsci.2016.02.007

Ali, A. M., Radwan, A. E., Abd El-Gawad, E. A., and Abdel-Latief, A. A. (2022). 3D integrated structural, facies and petrophysical static modeling approach for complex sandstone reservoirs: A case study from the coniacian–santonian matulla formation, july oilfield, gulf of suez, Egypt. *Nat. Resour. Res.* 31, 385–413. doi:10.1007/s11053-021-09980-9

Alsharhan, A. S., and Salah, M. G. (1995). Geology and hydrocarbon habitat in rift setting: northern and central gulf of suez, Egypt. *Bull. Can. Petroleum Geol.* 43 (2), 156–176.

Alsharhan, A. S. (2003). Petroleum geology and potential hydrocarbon plays in the Gulf of Suez rift basin, Egypt. *Am. Assoc. Pet. Geol. Bull.* 87 (1), 143–180. doi:10.1306/062002870143

Altmann, J. B., Müller, B. I. R., Müller, T. M., Heidbach, O., Tingay, M. R. P., and Weißhardt, A. (2014). Pore pressure stress coupling in 3D and consequences for reservoir stress states and fault reactivation. *Geothermics* 52, 195–205. doi:10.1016/j.geothermics.2014.01.004

Anderson, R. A., Ingram, D. S., and Zanier, A. M. (1973). Determining fracture pressure gradients from well logs. *J. Petroleum Technol.* 25 (11), 1259–1268. doi:10.2118/4135-pa

Attia, M., Abudeif, A., and Radwan, A. (2015). Petrophysical analysis and hydrocarbon potentialities of the untested middle Miocene Sidri and Baba sandstone of Belayim Formation, Badri field, gulf of suez, Egypt. *J. Afr. Earth Sci.* 109, 120–130. doi:10.1016/j.jafrearsci.2015.05.020

Audet, D. M., and McConnell, J. D. C. (1992). Forward modelling of porosity and pore pressure evolution in sedimentary basins. *Basin Res.* 4, 147–162. doi:10.1111/j.1365-2117.1992.tb00137.x

Bachrach, R., Noeth, S., Banik, N., Sengupta, M., Bunge, G., Flack, B., et al. (2007). From pore-pressure prediction to reservoir characterization: A combined geomechanics-seismic inversion workflow using trend-kriging techniques in a deepwater basin. *Lead. Edge* 26 (5), 590–595. doi:10.1190/1.2737099

Baouche, R., Sen, S., and Ganguli, S. S. (2020a). Pore pressure and *in-situ* stress magnitudes in the Bhiret Hammou hydrocarbon field, Berkine Basin, Algeria. *J. Afr. Earth Sci.* 171, 103945. doi:10.1016/j.jafrearsci.2020.103945

Baouche, R., Sen, S., and Boutaleb, K. (2020b). Distribution of pore pressure and fracture pressure gradients in the paleozoic sediments of Takouazet field, Illizi basin, Algeria. *J. Afr. Earth Sci.* 164, 103778. doi:10.1016/j.jafrearsci.2020.103778

Barakat, A. O., Mostafa, A., El-Gayar, M. S., and Rullkötter, J. (1997). Source-dependent biomarker properties of five crude oils from the Gulf of Suez, Egypt. Org. *Geochem* 26 (7-8), 441–450.

Barakat, A. O., Mostafa, A. R., Qian, Y., and Kennicutt Ii, M. C. (2002). Application of petroleum hydrocarbon chemical fingerprinting in oil spill investigations–-Gulf of Suez, Egypt. *Spill Sci. Technol. Bull.* 7 (5-6), 229–239. doi:10.1016/s1353-2561(02)00039-7

Bentley, B. B., and Biller, E. J. (1990). "Exploitation study and impact on the Kareem Formation, south EI morgan field, gulf of suez, Egypt," in Offshore Technology Conference, Houston, Texas, May 7–10, 1990.

Berhmann, J. H., Flemings, P. B., and John, C. M. (2006). Rapid sedimentation, overpressure, and focused fluid flow, Gulf of Mexico continental margin. *Sci. Dril.* 3, 12–17. doi:10.5194/sd-3-12-2006

Bjørlykke, K., Jahren, J., Aagaard, P., and Fisher, Q. (2010). Role of effective permeability distribution in estimating overpressure using basin modelling. *Mar. Pet. Geol.* 27 (8), 1684–1691. doi:10.1016/j.marpetgeo.2010.05.003

Borge, H. (2002). Modelling generation and dissipation of overpressure in sedimentary basins: an example from the halten terrace, offshore Norway. *Mar. Pet. Geol.* 19 (3), 377–388. doi:10.1016/s0264-8172(02)00023-5

Bosworth, W., and Durocher, S. (2017). Present-day stress fields of the gulf of suez (Egypt) based on exploratory well data: non-uniform regional extension and its relation to inherited structures and local plate motion. *J. Afr. Earth Sci.* 136, 136–147. doi:10.1016/JjafrearSci2017.04.025

Bosworth, W., and McClay, K. R. (2001). *Structural and stratigraphic evolution of the neogene Gulf of Suez, Egypt: a synthesis, 369*. Peritethyan rift/wrench basins and passive margins: Memoires du Museum National d'Historie Naturelle de Paris: Peritethys Programme (PTP) and International Geological Correlation Program (IGCP). Paris: Illustration 186, 567–606.

Bosworth, W., and Taviani, M. (1996). Late quaternary reorientation of stress field and extension direction in the southern gulf of suez, Egypt: evidence from uplifted coral terraces, mesoscopic fault arrays, and borehole breakouts. *Tectonics* 15, 791–802. doi:10.1029/95tc03851

Bosworth, W., Crevello, P., Winn, R. D., and Steinmetz, J. (1998). "Structure, sedimentation, and basin dynamics during rifting of the Gulf of Suez and north-western Red Sea," in *Sedimentation and tectonics in rift basins red sea:-gulf of aden* (Dordrecht: Springer), 77–96.

Bourgoyne, A. T., Millheim, K. K., Chenevert, M. E., and Young, F. S. (1986). *Applied drilling engineering*. United States: Society of Petroleum Engineers.

Bourgoyne, A. T., Jr, Millheim, K. K., Chenevert, M. E., and Young, F. S., Jr (1991). *Applied drilling engineering*. United States: Society of Petroleum Engineers.

Bowers, G. L. (2001). "Determining an appropriate pore-pressure estimation strategy," in Offshore technology conferenceHouston, Texas, April 30–May 3, 2001.

Brahma, J., Sircar, A., and Karmakar, G. P. (2013). Pre-drill pore pressure prediction using seismic velocities data on flank and synclinal part of Atharamura anticline in the Eastern Tripura, India. *J. Pet. Explor. Prod. Technol.* 3 (2), 93–103. doi:10.1007/s13202-013-0055-0

Brown, R. N. (1980). *History of exploration and discovery of morgan, ramadan and july oilfields, Gulf of Suez, Egypt*. Report. Available at: https://archives.datapages.com/data/cspg_sp/data/006/006001/733_cspgsp0060733.htm

Burgreen-Chan, B., Meisling, K. E., and Graham, S. (2015). Basin and petroleum system modelling of the east coast basin, New Zealand: a test of overpressure scenarios in a convergent margin. *Basin Res.* 28, 536–567. doi:10.1111/bre.12121

Carcione, J. M., and Gangi, A. F. (2000). Gas generation and overpressure: Effects on seismic attributes. *Geophysics* 65 (6), 1769–1779. doi:10.1190/1.1444861

Charts, S. (1991). *Log interpretation charts*. Houston, Texas, USA: Schlumberger.

Chen, X., Cao, W., Gan, C., and Wu, M. (2022). A hybrid spatial model based on identified conditions for 3D pore pressure estimation. *J. Nat. Gas Sci. Eng.* 100, 104448. doi:10.1016/j.jngse.2022.104448

Chi, G., Lavoie, D., Bertrand, R., and Lee, M. K. (2010). Downward hydrocarbon migration predicted from numerical modeling of fluid overpressure in the Paleozoic Anticosti Basin, Eastern Canada. *Geofluids* 10, 334–350. doi:10.1111/j.1468-8123.2010.00280.x

Chopra, S., and Huffman, A. R. (2006). Velocity determination forpore-pressure prediction: The Lead. *Lead. Edge* 25 (12), 1502–1515. doi:10.1190/1.2405336

Couzens-Schultz, B. A., and Azbel, K. (2014). Predicting pore pressure in active fold–thrust systems: An empirical model for the deepwater Sabah foldbelt. *J. Struct. Geol.* 69, 465–480. doi:10.1016/j.jsg.2014.07.013

Daniel, R. B. (2001). Pressure prediction for a central graben wildcat well, UK North Sea. *Mar. Pet. Geol.* 18 (2), 235–250. doi:10.1016/s0264-8172(00)00057-x

Darby, D., Haszeldine, R. S., and Couples, G. D. (1998). Central North Sea overpressures: insights into fluid flow from one- and two-dimensional basin modelling. *Geol. Soc. Spec. Publ.* 141 (1), 95–107. doi:10.1144/gsl.sp.1998.141.01.06

Das, B., and Chatterjee, R. (2018a). Mapping of pore pressure, *in-situ* stress and brittleness in unconventional shale reservoir of krishna-godavari basin. *J. Nat. Gas. Sci. Eng.* 50, 74–89. doi:10.1016/j.jngse.2017.10.021

Das, B., and Chatterjee, R. (2018b). Well log data analysis for lithology and fluid identification in Krishna-Godavari Basin, India. *Arab. J. Geosci.* 11, 231–242. doi:10.1007/s12517-018-3587-2

Dasgupta, S., Chatterjee, R., and Mohanty, S. P. (2016). Prediction of pore pressure and fracture pressure in Cauvery and Krishna-Godavari basins, India. *Mar. Pet. Geol.* 78, 493–506. doi:10.1016/j.marpetgeo.2016.10.004

Dasgupta, S., Chatterjee, R., Mohanty, S. P., and Alam, J. (2019). Pore pressure modeling in a compressional setting: A case study from Assam, NE India. *J. Petroleum Geol.* 42 (3), 319–338. doi:10.1111/jpg.12736

Draou, A., and Osisanya, S. O. (2000). "New methods for estimating of formation pressures and fracture gradients from well logs," in SPE Annual Technical Conference and Exhibition, Dallas, Texas, October 1–4, 2000.

Drews, M. C., Bauer, W., Caracciolo, L., and Stollhofen, H. (2018). Disequilibrium compaction overpressure in shales of the bavarian foreland molasse basin: results and geographical distribution from velocity-based analyses. *Mar. Pet. Geol.* 92, 37–50. doi:10.1016/j.marpetgeo.2018.02.017

Drews, M. C., Hofstetter, P., Zosseder, K., Straubinger, R., Gahr, A., and Stollhofen, H. (2019). Retracted article: Predictability and controlling factors of overpressure in the north alpine foreland basin, SE Germany: an interdisciplinary post-drill analysis of the geretsried GEN-1 deep geothermal well. *Geotherm. Energy* 7 (1), 3. doi:10.1186/s40517-019-0121-z

Duppenbecker, J. S., Illife, J., Osborne, M. J., and Harrold, T., (2004). "The role of multi-dimensional basin modeling in integrated pre- drill pressure prediction". AAPG/SEPM Conference on Basin Modeling. In Paper presented on 11th meeting of the Geologic Modelling Society, Galveston (Vol. 5).

Dutta, N. C. (2002). Geopressure prediction using seismic data: Current status and the road ahead. *Geophysics* 67 (6), 2012–2041. doi:10.1190/1.1527101

Eaton, B. A. (1975). "The equation for geopressure prediction from well logs," in *Fall meeting of the society of petroleum engineers of AIME* (United States: Society of Petroleum Engineers).

EGPC (1996). *Gulf of Suez oil fields (a comprehensive overview)*. Cairo: Egyptian General Petroleum Corporation, 736.

El Ayouty, M. K. (2017). "Petroleum geology," in *The geology of Egypt* (England: Routledge), 567–600.

El Diasty, W. S., and Peters, K. E. (2014). Genetic classification of oil families in the central and southern sectors of the Gulf of Suez, Egypt. *J. Petroleum Geol.* 37 (2), 105–126. doi:10.1111/jpg.12573

El Nady, M. M. (2006). The hydrocarbon potential of Miocene source rocks for oil generation in the South Gulf of Suez, Egypt. *Pet. Sci. Technol.* 24 (5), 539–562. doi:10.1081/lft-200041125

El-Ashry, M. T. (1972). Source and dispersal of reservoir sands in El morgan field, gulf of suez, Egypt. *Sediment. Geol.* 8 (4), 317–325. doi:10.1016/0037-0738(72)90047-4

El-Hattab, M. I. (1982). GUPCO'S experience in treating gulf of suez seawater for waterflooding the El Morgan oil field. *J. Petroleum Technol.* 34 (07), 1449–1460. doi:10.2118/10090-pa

Ganguli, S. S., and Sen, S. (2020). Investigation of present-day *in-situ* stresses and pore pressure in the south Cambay Basin, western India: Implications for drilling, reservoir development and fault reactivation. *Mar. Pet. Geol.* 118, 104422. doi:10.1016/j.marpetgeo.2020.104422

Ganguli, S. S., Vedanti, N., Pandey, O. P., and Dimri, V. P. (2018). Deep thermal regime, temperature induced over-pressured zone and implications for hydrocarbon potential in the Ankleshwar oil field, Cambay basin, India. *J. Asian Earth Sci.* 161, 93–102. doi:10.1016/j.jseaes.2018.05.005

Gardner, G. H. F., Gardner, L., and Gregory, A. (1974). Formation velocity and density—the diagnostic basics for stratigraphic traps. *Geophysics* 39 (6), 770–780. doi:10.1190/1.1440465

Gawad, W. A., Gaafar, I., and Sabour, A. A., (1986). Miocene stratigraphic nomenclature in the Gulf of Suez region. In: Egyptian General Petroleum Corporation, 8th Exploration Conference, Cairo, 1–20.

Gordon, D. S., and Flemings, P. B. (1998). Generation of overpressure and compaction-driven fluid flow in a Plio-Pleistocene growth-faulted basin, Eugene Island 330, offshore Louisiana. *Basin Res.* 10 (2), 177–196. doi:10.1046/j.1365-2117.1998.00052.x

Grauls, D. J., and Baleix, J. M. (1993). Role of overpressures and *in-situ* stresses in fault controlled hydrocarbon migration: a case study. *Mar. Pet. Geol.* 11, 734–742. doi:10.1016/0264-8172(94)90026-4

Gray-Stephens, D., Cook, J. M., and Sheppard, M. C. (1994). Influence of pore pressure on drilling response in hard shales. *SPE Drill. Complet.* 9 (04), 263–270. doi:10.2118/23414-pa

Gretener, P. E. (1979). *Pore pressure: fundamentals, general ramifications and implications for structural geology*. United States: American Association of Petroleum Geologists. revised edition.

Gutierrez, M., and Wangen, M. (2005). Modeling of compaction and overpressuring in sedimentary basins. *Mar. Pet. Geol.* 22, 351–363. doi:10.1016/j.marpetgeo.2005.01.003

Gutierrez, M. A., Braunsdor, N. R., and Couzens, B. A. (2006). Calibration and ranking of pore-pressure prediction models. *Lead. Edge* 25 (12), 1516–1523. doi:10.1190/1.2405337

Hansom, J., and Lee, M. K. (2005). Effects of hydrocarbon generation, basal heat flow and sediment compaction on overpressure development: a numerical study. *Pet. Geosci.* 11 (4), 353–360. doi:10.1144/1354-079304-651

Hao, F., Cai, D. S., Zou, H. Y., Fang, Y., and Zeng, Z. P. (2004). Overpressure-tectonic activity controlled fluid flow and rapid petroleum accumulation in Bozhong Depression, Bohai Bay basin. *Earth Sci.* 29 (9), 518–524.

Harrison, W. J., and Summa, L. L. (1991). Paleohydrology of the gulf of Mexico basin. *Am. J. Sci.* 291 (2), 109–176. doi:10.2475/ajs.291.2.109

Hart, B. S., Flemings, P. B., and Deshpande, A. (1995). Porosity and pressure: Role of compaction disequilibrium in the development of geopressures in a Gulf Coast Pleistocene basin. *Geol.* 23 (1), 45–48. doi:10.1130/0091-7613(1995)023<0045:paproc>2.3.co;2

He, S., Middleton, M., Kaiko, A., Jiang, C., and Li, M. (2002). Two case studies of thermal maturity and thermal modelling within the overpressured Jurassic rocks of the Barrow Sub-basin, North West Shelf of Australia. *Mar. Pet. Geol.* 19 (2), 143–159. doi:10.1016/s0264-8172(02)00006-5

Helset, H. M., Lüthje, M., and Ojala, I. (2009). "Improved pore pressure prediction by integrating basin modeling and seismic methods," in Basin and Petroleum System Modeling: New Horizons in Research and Applications (AAPG Hedberg Research Conference in Napa, California), Napa, California, May 3-8, 2009.

Hillis, R. (2000). Pore pressure/stress coupling and its implications for seismicity. *Explor. Geophys.* 31 (2), 448–454. doi:10.1071/eg00448

Hoesni, M. J. (2004). "Origins of overpressure in the Malay Basin and its influence on petroleum systems," (Durham University). Doctoral dissertation.

Hughes, S. C., Ahmed, H., and Raheem, T. A. (1997). "Exploiting the mature south El morgan Kareem reservoir for yet more oil: a case study on multi-discipline reservoir management," in Middle East Oil Show and Conference, Bahrain, March 1997. doi:10.2118/37783-MS

Hussain, M., and Ahmed, N. (2018). Reservoir geomechanics parameters estimation using well logs and seismic reflection data: insight from sinjhoro field, lower indus basin, Pakistan. *Arab. J. Sci. Eng.* 43 (7), 3699–3715. doi:10.1007/s13369-017-3029-6

Jackson, Ch.A. L., Gawthorpe, R. L., Leppard, Ch., and Sharp, I. (2006). Rift-initiation development of normal fault blocks: Insights from the Hammam Faraun fault block, Suez Rift, Egypt. *J. Geol. Soc. Lond.* 163 (1), 165–183. doi:10.1144/0016-764904-164

Jafarizadeh, F., Rajabi, M., Tabasi, S., Seyedkamali, R., Davoodi, S., Ghorbani, H., et al. (2022). Data driven models to predict pore pressure using drilling and petrophysical data. *Energy Rep.* 8, 6551–6562. doi:10.1016/j.egyr.2022.04.073

Jeans, C. V. (1994). Clay diagenesis, overpressure and reservoir quality: an introduction. *Clay Min.* 29 (4), 415–423. doi:10.1180/claymin.1994.029.4.02

John, A., Kumar, A., and Gupta, P. (2014). An integrated pore-pressure model and its application to hydrocarbon exploration: A case study from the mahanadi basin, east coast of India. *Interpretation* 2 (1), SB17–SB26. doi:10.1190/int-2013-0078.1

Karlsen, D. A., and Skeie, J. E. (2006). Petroleum migration, faults and overpressure, part I: calibrating basin modeling using petroleum in traps—a review. *J. Pet. Geol.* 29 (3), 227–256. doi:10.1111/j.1747-5457.2006.00227.x

Kassem, A. A., Sen, S., Radwan, A. E., Abdelghany, W. K., and Abioui, M. (2021). Effect of depletion and fluid injection in the mesozoic and paleozoic sandstone reservoirs of the october oil field, central gulf of Suez basin: Implications on drilling, production and reservoir stability. *Nat. Resour. Res.* 30 (3), 2587–2606. doi:10.1007/s11053-021-09830-8

Katahara, K. (2006). "Overpressure and shale properties: Stress unloading or smectite-illite transformation?," in *SEG technical program expanded abstracts 2006* (Texas: Society of Exploration Geophysicists), 1520–1524.

Khalil, B., and Meshrif, W. M. (1988). "Hydrocarbon occurrences and structural style of the southern Suez Rift Basin, Egypt," in 9th Petroleum Exploration and Production Conference, Cairo, 86–109.

Khan, K. A., Bangash, A. A., and Akhter, G. (2017). Raw seismic velocities aid predictions in mud program designs. *Oil Gas J.* 115 (11), 30–35.

Klaus, B. (1999). Mechanisms for generating overpressure in sedimentary basin: A revaluation: 510 discussion. *AAPG Bull.* 83 (5), 798–800.

Kumar, R. R., and Rao, D. G. (2012). "Overpressure mechanisms in deep drilling in western offshore India," in AAPG International Conference and Exhibition, Singapore, September, 16–19.

Kutasov, I. M., and Eppelbaum, L. V. (2005). Determination of formation temperature from bottom-hole temperature logs—a generalized Horner method. *Journal of Geophysics and Engineering* 2 (2), 90–96.

Lahann, R. W., and Swarbrick, R. E. (2011). Overpressure generation by load transfer following shale framework weakening due to smectite diagenesis. *Geofluids* 11 (4), 362–375. doi:10.1111/j.1468-8123.2011.00350.x

Lahann, R. W., Lahann, W., McCarty, D. K., and Hsieh, J. C. C. (2001). "Influence of clay diagenesis on shale velocities and fluid-pressure," in *Offshore technology conference*.

Law, B. E., and Spencer, C. W. (1998). *Memoir 70, chapter 1: Abnormal pressure in hydrocarbon environments*. United States: American Association of Petroleum Geologists.

Lee, S., Shaw, J., Ho, R., Burger, J., Singh, S., and Troyer, B. (1999). Illuminating the shadows: tomography, attenuation and pore pressure processing in the south caspian sea. *J. Pet. Sci. Eng.* 24, 1–12. doi:10.1016/s0920-4105(99)00019-4

Li, C., Zhang, L., Luo, X., Lei, Y., Yu, L., Cheng, M., et al. (2021). Overpressure generation by disequilibrium compaction or hydrocarbon generation in the Paleocene Shahejie Formation in the Chezhen Depression: Insights from logging responses and basin modeling. *Mar. Petroleum Geol.* 133, 105258. doi:10.1016/j.marpetgeo.2021.105258

Li, C., Zhang, L., Luo, X., Wang, B., Lei, Y., Cheng, M., et al. (2022). Modeling of overpressure generation–evolution of the paleogene source rock and implications for the linnan sag, eastern China. *Front. Earth Sci. (Lausanne).* 10, 829322. doi:10.3389/feart.2022.829322

López, J. L., Rappold, P. M., Ugueto, G. A., Wieseneck, J. B., and Vu, C. K. (2004). Integrated shared earth model: 3D pore-pressure prediction and uncertainty analysis. *Lead. Edge* 23 (1), 52–59. doi:10.1190/1.1645455

Luo, X. R., and Vasseur, G. (1996). Geopressuring mechanism of organicmatter cracking: numerical modeling. *AAPG Bull.* 80, 856–874.

Luo, X., Wang, Z., Zhang, L., Yang, W., and Liu, L. (2007). Overpressure generation and evolution in a compressional tectonic setting, the southern margin of Junggar Basin, northwestern China. *Am. Assoc. Pet. Geol. Bull.* 91 (8), 1123–1139. doi:10.1306/02260706035

Mahetaji, M., Brahma, J., and Sircar, A. (2019). Pre-drill pore pressure prediction and safe well design on the top of tulamura anticline, Tripura, India: a comparative study. *J. Pet. Explor Prod. Technol.*, 1–29. doi:10.1007/s13202-019-00816-0

Mahmoud, S., Reilinger, R., McClusky, S., Vernant, P., and Tealeb, A. (2005). GPS evidence for northward motion of the Sinai block: implications for E Mediterranean tectonics. *Earth Planet. Sci. Lett.* 238, 217–224. doi:10.1016/j.epsl.2005.06.063

Marín-Moreno, H., Minshull, T. A., and Edwards, R. A. (2013). A disequilibrium compaction model constrained by seismic data and application to overpressure generation in the Eastern Black Sea Basin. *Basin Res.* 25 (3), 331–347. doi:10.1111/bre.12001

Martinsen, R. S. (1994). *Summary of published literature on anomalous pressures: Implications for the study of pressure compartments*. United States: American Association of Petroleum Geologists.

Matthews, M. D. (2004). "Uncertainty-shale pore pressure from borehole resistivity," in Gulf Rocks 2004, the 6th North America Rock Mechanics Symposium (NARMS), Houston, Texas, June 2004. Paper Number: ARMA-04-551.

McPherson, B., and Garven, G. (1999). Hydrodynamics and overpressure mechanisms in the Sacramento basin, California. *Am. J. Sci.* 299, 429–466. doi:10.2475/ajs.299.6.429

Mello, U. T., and Karner, J. D. (1996). Development of sediment overpressure and its effect on thermal maturation: Application to the Gulf of Mexico basin. *AAPG Bulletin* 80 (9), 1367–1396. doi:10.1306/64ED9A42-1724-11D7-8645000102C1865D

Metwalli, M. H., Phllip, G., and Youssef, E. S. A. (1978). El-Morgan oil field as a major fault-blocks reservoir masked by the thick Miocene salt; a clue for deeper reserves of hydrocarbons in Gulf of Suez Petroleum Province, Egypt. *Acta Geol. Pol.* 28 (3), 389–314.

Metwalli, M. H., Philip, G., and Youssif, E. A. A. (1981). El Morgan oil field crude oil and cycles of oil generation, migration and accumulation in the Gulf of Suez petroleum province, AR, Egypt. *Acta Bot. Hung* 24 (2-4), 369–387.

Mondal, S., and Chatterjee, R. (2019). Quantitative risk assessment for optimum mud weight window design: A case study. *J. Petroleum Sci. Eng.* 176, 800–810. doi:10.1016/j.petrol.2019.01.101

Montenat, C., D'Estevou, P. O., Purser, B., Burollet, P. F., Jarrige, J. J., Orszag-Sperber, F., et al. (1988). Tectonic and sedimentary evolution of the gulf of suez and the northwestern red sea. *Tectonophysics* 153 (1-4), 161–177. doi:10.1016/0040-1951(88)90013-3

Mosca, F., Djordjevic, O., Hantschel, T., McCarthy, J., Krueger, A., Phelps, D., et al. (2018). Pore pressure prediction while drilling: Three-dimensional earth model in the Gulf of Mexico. *Am. Assoc. Pet. Geol. Bull.* 102 (4), 691–708. doi:10.1306/0605171619617050

Mouchet, J. P., and Mitchele, A. (1989). "Abnormal pressures while drilling-Origins, prediction, detection, evaluation," in *Manuals techniques 2, elf aquitane edition* (Boussens: Editions TECHNIP), 253.

Moustafa, A. R., and Khalil, S. M. (2020). "Structural setting and tectonic evolution of the gulf of suez, NW red Sea and gulf of aqaba rift systems," in *The geology of Egypt* (Cham: Springer), 295–342.

Mudford, B. S., Gradstein, F. M., Katsube, T. J., and Best, M. E. (1991). Modelling 1D compaction-driven flow in sedimentary basins: a comparison of the scotian shelf, North Sea and gulf coast. *Geol. Soc. Spec. Publ.* 59 (1), 65–85. doi:10.1144/gsl.sp.1991.059.01.05

Nadeau, P. H. (1985). The physical dimensions of fundamental clay particles. *Clay Min.* 20 (4), 499–514. doi:10.1180/claymin.1985.020.4.06

Nagy, Z., Baracza, M. K., and Szabo, N. P. (2019). "Integrated pore pressure prediction with 3d basin modeling," in *Second EAGE workshop on pore pressure prediction*. doi:10.3997/2214-4609.201900513

Neuzil, C. E., and Pollock, D. W. (1983). Erosional unloading and fluid pressures in hydraulically "tight" rocks. *J. Geol.* 91, 179–193. doi:10.1086/628755

Neuzil, C. E. (1995). Abnormal pressures as hydrodynamic phenomena. *Am. J. Sci.* 295, 742–786. doi:10.2475/ajs.295.6.742

Nordgård Bolås, H. M., Hermanrud, C., and Teige, G. M. (2004). Origin of overpressures in shales: Constraints from basin modeling. *AAPG Bull.* 88 (2), 193–211. doi:10.1306/10060302042

O'Connor, S., Swarbrick, R., and Lahann, R. (2011a). Geologically-driven pore fluid pressure models and their implications for petroleum exploration. Introduction to thematic set. *Geofluids* 11 (4), 343–348. doi:10.1111/j.1468-8123.2011.00354.x

O'Connor, S., Swarbrick, R., Hoesni, J., and Lahann, R. (2011b). "Deep pore pressure prediction in challenging areas, Malay Basin, SE Asia," in Proceedings of Indonesia Petroleum Association, 35th Annual Convention and Exhibition.

Osborne, M. J., and Swarbrick, R. E. (1997). Mechanisms for generating overpressure in sedimentary basins: a reevaluation. *AAPG Bull.* 81 (6), 1023–1041.

Patton, T. L., Moustafa, A. R., Nelson, R. A., and Abdine, S. A. (1994). Tectonic evolution and structural setting of the Suez Rift: Chapter 1: Part I. Type Basin: Gulf of Suez.

Paul, S., Chatterjee, R., and Kundan, A. (2009). "Estimation of pore pressure gradient and fracture gradient from well logs: A theoretical analysis of techniques in use," in Indian Oil & Gas Review Symposium and International Exhibition (IORS-2009), Mumbai, India, September 11-12.

Peters, K. E., Schenk, O., Scheirer, A. H., Wygrala, B., and Hantschel, T. (2017). "Basin and petroleum system modeling," in *Springer handbook of petroleum technology* (Cham: Springer), 381–417.

Plumb, R. A., Evans, K. F., and Engelder, T. (1991). Geophysical log responses and their correlation with bed-to-bed stress contrasts in Paleozoic rocks, Appalachian Plateau, New York. *J. Geophys. Res.* 91, 14509–14528. doi:10.1029/91jb00896

Poelchau, H. S., Baker, D. R., Hantschel, T., Horsfield, B., and Wygrala, B. (1997). "Basin simulation and the design of the conceptual basin model," in *Petroleum and basin evolution* (Berlin, Heidelberg: Springer), 3–70.

Prosser, S. (1993). Rift-related linked depositional systems and their seismic expression. *Geological Society, London, Special Publications* 71 (1), 35–66.

Radwan, A., and Sen, S. (2021a). Stress path analysis for characterization of *in situ* stress state and effect of reservoir depletion on present-day stress magnitudes: Reservoir geomechanical modeling in the gulf of Suez Rift basin, Egypt. *Nat. Resour. Res.* 30, 463–478. doi:10.1007/s11053-020-09731-2

Radwan, A., and Sen, S. (2021b). Characterization of *in-situ* stresses and its implications for production and reservoir stability in the depleted El Morgan hydrocarbon field, Gulf of Suez Rift Basin, Egypt. *J. Struct. Geol.* 148, 104355. doi:10.1016/j.jsg.2021.104355

Radwan, A. E., Abudeif, A. M., Attia, M. M., and Mahmoud, M. A. (2019a). Development of formation damage diagnosis workflow, application on Hammam

Faraun reservoir: A case study, gulf of suez, Egypt. *J. Afr. Earth Sci.* 153, 42–53. doi:10.1016/j.jafrearsci.2019.02.012

Radwan, A. E., Abudeif, A. M., Attia, M. M., and Mohammed, M. A. (2019b). Pore and fracture pressure modeling using direct and indirect methods in Badri Field, Gulf of Suez, Egypt. *J. Afr. Earth Sci.* 156, 133–143. doi:10.1016/j.jafrearsci.2019.04.015

Radwan, A. E., Abudeif, A., Attia, M., and MahmouD, M. (2019c). "Formation damage diagnosis, application on Hammam Faraun reservoir: A case study, gulf of suez, Egypt," in Offshore Mediterranean Conference. doi:10.13140/RG.2.2.22352.66569

Radwan, A. E., Abudeif, A. M., Attia, M. M., Elkhawaga, M. A., Abdelghany, W. K., and Kasem, A. A. (2020a). Geopressure evaluation using integrated basin modelling, well-logging and reservoir data analysis in the northern part of the Badri oil field, Gulf of Suez, Egypt. *J. Afr. Earth Sci.* 162, 103743. doi:10.1016/j.jafrearsci.2019.103743

Radwan, A. E., Kassem, A. A., and Kassem, A. (2020b). Radwany formation: A new formation name for the early-middle Eocene carbonate sediments of the offshore october oil field, gulf of suez: Contribution to the Eocene sediments in Egypt. *Mar. Pet. Geol.* 116, 104304. doi:10.1016/j.marpetgeo.2020.104304

Radwan, A. E., Abudeif, A. M., and Attia, M. M. (2020c). Investigative petrophysical fingerprint technique using conventional and synthetic logs in siliciclastic reservoirs: A case study, gulf of Suez basin, Egypt. *J. Afr. Earth Sci.* 167, 103868. doi:10.1016/j.jafrearsci.2020.103868

Radwan, A. E., Trippetta, F., Kassem, A. A., and Kania, M. (2021a). Multi-scale characterization of unconventional tight carbonate reservoir: Insights from October oil filed, Gulf of Suez rift basin, Egypt. *J. Petroleum Sci. Eng.* 197, 107968. doi:10.1016/j.petrol.2020.107968

Radwan, A. E., Nabawy, B. S., Kassem, A. A., and Hussein, W. S. (2021b). Implementation of rock typing on waterflooding process during secondary recovery in oil reservoirs: A case study, El morgan oil field, gulf of suez, Egypt. *Nat. Resour. Res.* 30, 1667–1696. doi:10.1007/s11053-020-09806-0

Radwan, A. E., Rohais, S., and Chiarella, D. (2021c). Combined stratigraphic-structural play characterization in hydrocarbon exploration: a case study of middle Miocene sandstones, gulf of Suez basin, Egypt. *J. Asian Earth Sci.* 218, 104686. doi:10.1016/j.jseaes.2021.104686

Radwan, A. E., Abdelghany, W. K., and Elkhawaga, M. A. (2021d). Present-day *in-situ* stresses in Southern Gulf of Suez, Egypt: Insights for stress rotation in an extensional rift basin. *J. Struct. Geol.* 147, 104334. doi:10.1016/j.jsg.2021.104334

Radwan, A. E., Wood, D. A., Abudeif, A. M., Attia, M. M., Mahmoud, M., Kassem, A. A., et al. (2021e). Reservoir formation damage; reasons and mitigation: A case study of the cambrian–ordovician nubian 'C' sandstone gas and oil reservoir from the gulf of Suez Rift basin. *Arab. J. Sci. Eng.* doi:10.1007/s13369-021-06005-8

Radwan, A. E., Wood, D. A., and Radwan, A. A. (2022). Machine learning and data-driven prediction of pore pressure from geophysical logs: A case study for the mangahewa gas field, New Zealand. *J. Rock Mech. Geotechnical Eng.* doi:10.1016/j.jrmge.2022.01.012

Radwan, A. E. (2014). "Petrophysical evaluation for Sidri and Baba members within Belayim Formation in the region of Badri field, gulf of suez, Egypt,". M.Sc. Thesis. doi:10.13140/RG.2.2.22772.09601

Radwan, A. E. (2018). "New petrophysical approach and study of the pore pressure and formation damage in Badri, Morgan and Sidki fields, Gulf of Suez Region Egypt,". PhD Thesis. doi:10.13140/RG.2.2.26651.82727

Radwan, A. E. (2021a). Modeling the depositional environment of the sandstone reservoir in the middle Miocene Sidri member, Badri field, gulf of Suez basin, Egypt: Integration of gamma-ray log patterns and petrographic characteristics of lithology. *Nat. Resour. Res.* 30, 431–449. doi:10.1007/s11053-020-09757-6

Radwan, A. E. (2021b). Modeling pore pressure and fracture pressure using integrated well logging, drilling based interpretations and reservoir data in the Giant El Morgan oil Field, Gulf of Suez, Egypt. *J. Afr. Earth Sci.* 178, 104165. doi:10.1016/j.jafrearsci.2021.104165

Radwan, A. E. (2021c). Integrated reservoir, geology, and production data for reservoir damage analysis: A case study of the Miocene sandstone reservoir, gulf of suez, Egypt. *Interpretation* 9 (4), SH27–SH37. doi:10.1190/int-2021-0039.1

Radwan, A. E. (2022a). "Chapter Two - three-dimensional gas property geological modeling and simulation," in *Sustainable geoscience for natural gas sub-surface systems*. Editors D. A. Wood and J. Cai (Netherlands: Elsevier), 29–45. Chapter 2 in. doi:10.1016/B978-0-323-85465-8.00011-X

Radwan, A. E. (2022b). Provenance, depositional facies, and diagenesis controls on reservoir characteristics of the middle Miocene tidal sandstones, gulf of Suez Rift basin : integration of petrographic analysis and gamma-ray log patterns. *Environ. Earth Sci.* 81 (15), 382. doi:10.1007/s12665-022-10502-w

Ramdhan, A. M., and Goulty, N. R. (2010). Overpressure-generating mechanisms in the peciko field, lower kutai basin, Indonesia. *Pet. Geosci.* 16 (4), 367–376. doi:10.1144/1354-079309-027

Ramdhan, A. M., and Goulty, N. R. (2011). Overpressure and mudrock compaction in the lower kutai basin, Indonesia: A radical reappraisal. *Am. Assoc. Pet. Geol. Bull.* 95 (10), 1725–1744. doi:10.1306/02221110094

Rashed, A. (1990). "The main fault trends in the Gulf of Suez and their role in oil entrapment," in 10th Petroleum Exploration and Production Conference, Cairo, 1–24.

Robson, D. A. (1971). The structure of the Gulf of Suez (Clysmic) rift, with special reference to the eastern side. *J. Geol. Soc. Lond.* 127 (3), 247–271. doi:10.1144/gsjgs.127.3.0247

Rohrback, B. G. (1982). "Crude oil geochemistry of the gulf of suez: Egyptian general petroleum corporation," in 6th International Exploration Conference, Cairo.

Satti, I. A., Ghosh, D., and Yusoff, W. I. W. (2015). 3D predrill pore pressure prediction using basin modeling approach in a field of Malay Basin. *Asian J. Earth Sci.* 8, 24–31. doi:10.3923/ajes.2015.24.31

Sayers, C. M., Johnson, G. M., and Denyer, G. (2002). Predrill pore-pressure prediction using seismic data. *Geophysics* 67 (4), 1286–1292. doi:10.1190/1.1500391

Schutz, K. I. (1994). "Structure and stratigraphy of the gulf of suez, Egypt: Chapter 2: Part I," in *Type basin: Gulf of Suez*. Available at: https://archives.datapages.com/data/specpubs/basinar3/data/a137/a137/0001/0050/0057.htm

Selim, S. M., and Badawy, B. E. S. (2010). "Pressure regime evaluation, role and contribution in well planning," in *Zeit bay field, Gulf of Suez* (Egypt.

Selim, S. M., El-Badawy, B. A., Allah, K. M. A., and Khorshid, A. (2003). "Role and contribution of pressure regime modeling in well planning and formation evaluation process, gulf of suez oil fields, Egypt," in AAPG Annual Meeting 2003.

Sen, S., and Ganguli, S. S. (2019). "Estimation of pore pressure and fracture gradient in Volve field, Norwegian North Sea," in *SPE oil and gas India conference and exhibition* (United States: Society of Petroleum Engineers).

Sen, S., Corless, J., Dasgupta, S., Maxwell, C., and Kumar, M. (2017). "Issues faced while calculating overburden gradient and picking shale zones to predict pore pressure," in *First EAGE workshop on pore pressure prediction* (Netherlands: European Association of Geoscientists & Engineers), 506.

Sen, S., Kundan, A., Kalpande, V., and Kumar, M. (2019). The present-day state of tectonic stress in the offshore Kutch-Saurashtra Basin, India. *Mar. Pet. Geol.* 102, 751–758. doi:10.1016/j.marpetgeo.2019.01.018

Sen, S., Kundan, A., and Kumar, M. (2020). Modeling pore pressure, fracture pressure and collapse pressure gradients in offshore panna, western India: Implications for drilling and wellbore stability. *Nat. Resour. Res.* 29, 2717–2734. doi:10.1007/s11053-019-09610-5

Shaker, S. (2007). Calibration of geopressure predictions using the normal compaction trend: Perception and pitfall. *CSEG Rec.* 32, 29–35.

Shaker, S. S. (2015). A new approach to pore pressure predictions: Generation, expulsion, and retention trio—case histories from the Gulf of Mexico. *Gulf Coast Association of Geological Societies Transactions* 65 (2015), 323–337.

Singha, D. K., Chatterjee, R., Sen, M. K., and Sain, K. (2014). Pore pressure prediction in gas-hydrate bearing sediments of Krishna–Godavari basin, India. *Mar. Geol.* 357, 1–11. doi:10.1016/j.margeo.2014.07.003

Snee, J. E. L. (2015). "Predicting overpressure using basin modeling software," in *Reservoir Geomechanics* (Cambridge: Cambridge University Press).

Spencer, C. W. (1987). Hydrocarbon generation as a mechanism for overpressuring in Rocky Mountain region. *AAPG Bull.* 71 (4), 368–388.

Swarbrick, R. E., and Osborne, M. J. (1998). *Memoir 70, chapter 2: Mechanisms that generate abnormal pressures: an overview*.

Swarbrick, R. E. (2002). Developing pressure histories through basin modeling. *AAPG Bull.* 86 (13), 10–13.

Swarbrick, R. (2012). Review of pore-pressure prediction challenges in high-temperature areas. *Lead. Edge* 31 (11), 1288–1294. doi:10.1190/tle31111288.1

Tariq, Z., Mahmoud, M. A., Abdulraheem, A., Al-Nakhli, A., and BaTaweel, M. (2019). An experimental study to reduce the fracture pressure of high strength rocks using a novel thermochemical fracturing approach. *Geofluids* 2019, 1. doi:10.1155/2019/1904565

Thomsen, R. O. (1998). Aspects of applied basin modelling: sensitivity analysis and scientific risk. *Geol. Soc.* 141, 209–221. doi:10.1144/gsl.sp.1998.141.01.13

Tobin, R. C. (1997). *Porosity prediction in frontier basins: a systematic approach to estimating subsurface reservoir quality from outcrop samples*. United States: American Association of Petroleum Geologists.

Traugott, M. (1997). Pore/fracture pressure determinations in deep water. *World oil.* 218 (8), 68–70.

Vejbæk, O. V. (2008). Disequilibrium compaction as the cause for cretaceous–paleogene overpressures in the Danish North Sea. *Am. Assoc. Pet. Geol. Bull.* 92 (2), 165–180. doi:10.1306/10170706148

Wang, X., He, S., Wei, A., Liu, Q., and Liu, C. (2016). Typical disequilibrium compaction caused overpressure of paleocene dongying formation in northwest liaodongwan depression, bohai bay basin, China. *J. Petroleum Sci. Eng.* 147, 726–734. doi:10.1016/j.petrol.2016.09.014

Wessling, S., Bartetzko, A., and Tesch, P. (2013). Quantification of uncertainty in a multistage/multiparameter modeling workflow: Pore pressure from geophysical well logs. *Geophysics* 78 (3), WB101–WB112. doi:10.1190/geo2012-0402.1

Xie, X., Bethke, C. M., Li, S., Liu, X., and Zheng, H. (2001). Overpressure and petroleum generation and accumulation in the dongying depression of the bohaiwan basin, China. *Geofluids* 1 (4), 257–271. doi:10.1046/j.1468-8123.2001.00017.x

Yardley, G. S., and Swarbrick, R. E. (2000). Lateral transfer: A source of additional overpressure? *Mar. Pet. Geol.* 17 (4), 523–537. doi:10.1016/s0264-8172(00)00007-6

Yassir, N. A., and Bell, J. S. (1996). Abnormally high fluid pressures and associated porosities and stress regimes in sedimentary basins. *SPE Form. Eval.* 11 (01), 5–10. doi:10.2118/28139-pa

Youssef, E. A. A., Metwalli, M. H., Fattah, M. A., and Abu Shadi, F. (2002). "Diagenesis and reservoir quality evolution of the Miocene petroleum-bearing sandstones in Badr oil field, Gulf of Suez, Egypt," in Proceedings 6th International Conference on the Geology of the Arab World, Cairo, 757–778.

Zhang, J., He, S., Wang, Y., Wang, Y., Hao, X., Luo, S., et al. (2019). Main mechanism for generating overpressure in the paleogene source rock series of the chezhen depression, bohai bay basin, China. *J. Earth Sci.* 30, 775–787. doi:10.1007/s12583-017-0959-6

Zhang, J. (2011). Pore pressure prediction from well logs: Methods, modifications, and new approaches. *Earth. Sci. Rev.* 108 (1-2), 50–63. doi:10.1016/j.earscirev.2011.06.001

Glossary

AG air gap (foot)

D depth (foot)

EMW equivalent mud weight (ppg)

Fp fracture pressure (psi)

g gravitational acceleration (m/s^2)

H true vertical depth value at the point of investigation (foot)

NCT normal compaction trend

OBG overburden pressure gradient (ppg)

P hyd hydrostatic pressure (ppg)

P wellbore pressure (psi)

PP pore pressure (Ppg or psi)

ppfg pore pressure fracture gradient

ppg pound per gallon

PPN normal pore pressure gradient (or hydrostatic pressure) (ppg, psi)

RFT repeated formation test (ppg or psi)

RHOB bulk density log value (g/cc)

RN normal resistivity (ohm-meter)

Ro observed resistivity (ohm-meter)

TVD true vertical depth (foot)

Vs vertical stress (psi)

WD water depth (foot)

x Eaton exponent and its value is 1.2 for the resistivity and 3 for the sonic in Eaton, 1975. Values are 0.9 for the resistivity and 1.65 for the sonic in the Gulf of Suez (dimensionless)

α exponent coefficient (0.85, for the Gulf of Suez) (unitless)

ΔTN normal sonic (ms/ft)

ΔTo observed sonic (ms/ft)

ρ(H) bulk density of the overlying rock, represented as function of depth (H) (g/cc)

ρ_wg/cc ρ_w density of water column (taken as 1.02 g/cc)

σmudlineg/cm3 σmudline mud line density (2.15 g/cm3, for the Gulf of Suez

σVAmoco Amoco vertical stress (ppg)

ν Poisson's ratio. (Eaton, 1975, The used dynamic Poisson's ratio value in the Gulf of Suez region is 0.33). (Radwan et al. 2019b; Radwan et al. 2020a) (unitless)